Charge ordering in low dimensional organic compounds*

Pierre Monceau

Institut Néel, Grenoble, France

* in collaboration with Felix Nad+, Institut Kotel'nikov of Radioengineering and Electronics, RAS, Moscow, Russia
and S. Brazovski (LPTMS, Orsay, France)

Outline

- charge ordering (CO) in quasi-one and quasi-two dimensional organic compounds induces a ferroelectric polarization on the basis of observation of a divergent increase of the dielectric susceptibility at the CO transition temperature.

- for two-dimensional organic salts of general formula θ- (BEDT-TTF)$_2$X, the geometrical frustration caused by the triangular lattice prevents long range order, but competition between domains with different charge ordering yields possibly a glass-like short range charge order state at low temperature.

Half-filled band

In the case of half-filled band and strong Coulomb interactions between electrons (strong U) on neighouring sites, it is more favorable to localize the particules on the lattice sites to minimize the repulsion and the system is an insulator- the Mott transition

¼ filled band

The mean field approximation of the 1D Hubbard model shows that when V exceeds a critical value, V_c, , charge disproportionation occurs among sites with alternating « charge rich » and « charge poor » sites (Seo and Fukuyama 1997).

With $\Delta_D \neq 0$ numerical calculations on the plane U and V for a fixed Δ_D where the metallic phase at $\Delta_D = 0$ is replaced by the Mott insulating phase, and a phase with Wigner crystal-type CO is still present in the large U and V region

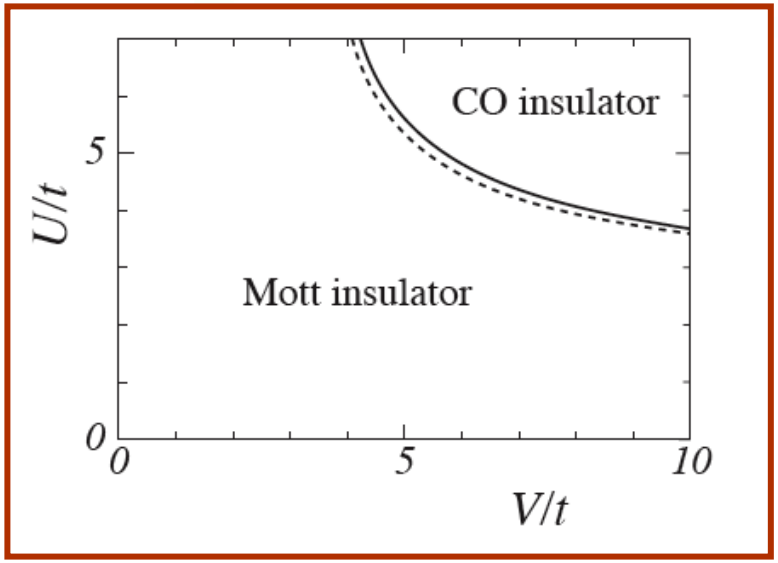

Ground state phase diagram of the 1D extended Hubbard model at 1/4 filling on the plane of U/t and V/t for a fixed value of the dimerization gap Δ_D

Shibata et al. Tsuchiizu et al. 2001

Quarter-filled without dimerization: DI-DCNQI)$_2$Ag Wigner crystal type of charge ordering
K.Hiraki and K. Kanoda, Phys. Rev. Lett. 80 (1998) 4737

Charge order and ferroelectricity in quasi-1D Fabre salts

Structure of Bechgaard-Fabre salts

C = S, Se

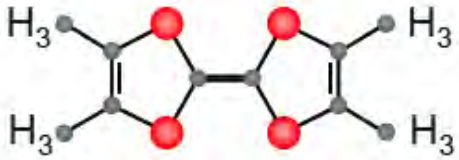

X = AsF_6, PF_6, ClO_4, BF_4, ...

parallel to the stacks (a-c plane)

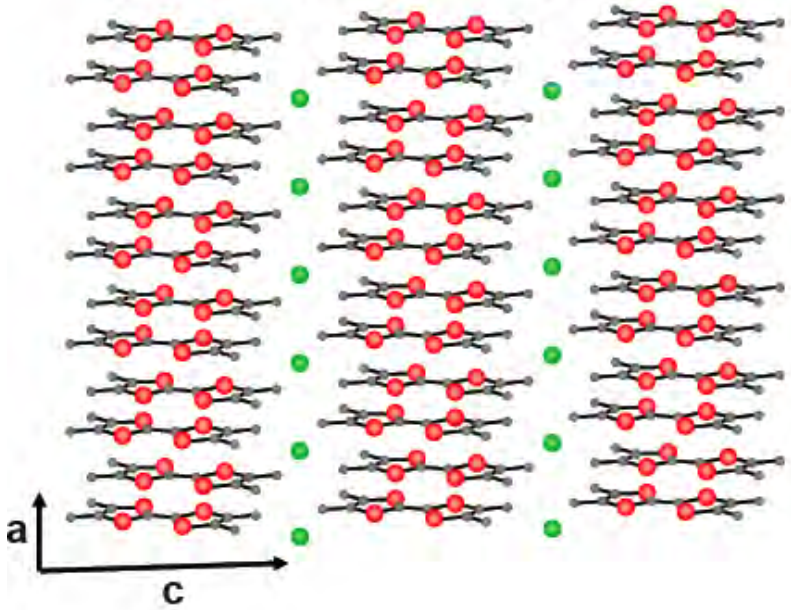

perpendicular to the stacks (b-c plane)

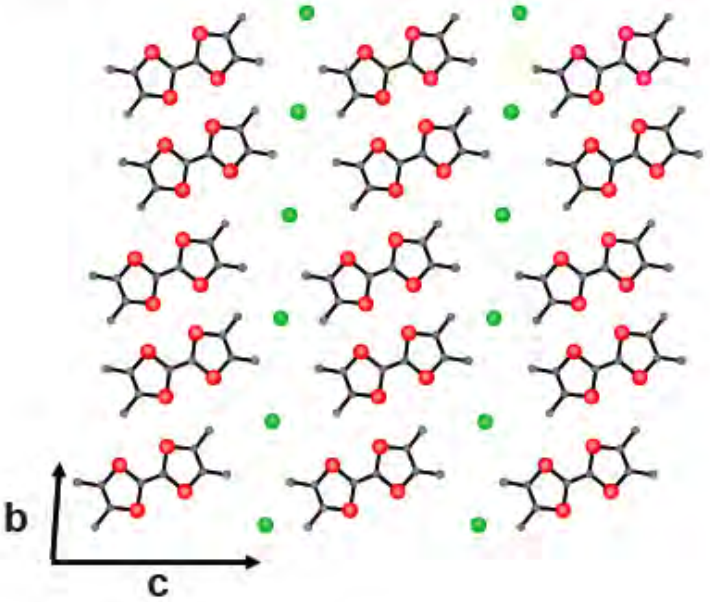

Phase diagramme

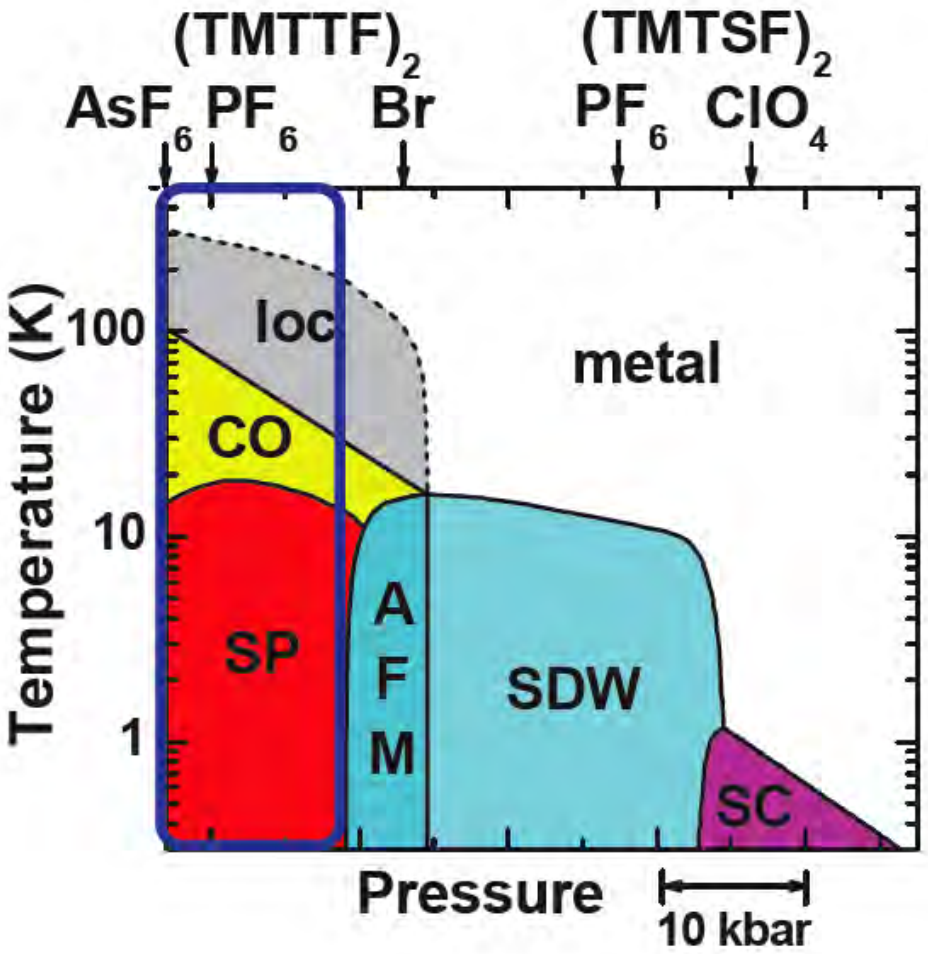

Symmetry of anions

Centrosymmetric anions (CSA)
spherical: Br^-
octahedral: PF_6,AsF_6,SbF_6^-

Non-centrosymmetric anions (NCSA)
tetrahedral:ClO_4,BF_4,ReO_4li
near: SCN^-

C.Bourbonnais and D.Jérome 1990

- Ferroelectricity is defined by the appearance of a macroscopic electric polarization and its reversibility by applying an external field

- For some ferroelectric materials, electron degrees of freedom and/or electronic interactions directly give rise to a macroscopic electric polarization and a ferroelectric transition $\Rightarrow$ electronic ferroelectricity

-**Spin-driven ferroelectricity** where the ferroelectric transition is caused by magnetic interactions and magnetic ordering (primary order parameter)

called multiferroics (cross-correlation between ferroelectricity and magnetism) Ex.:$TbMnO_3$ (for a review: T. Arima, J. Phys. Soc. Jpn 80, 052001, 2011)

-**Charge-ordered ferroelectricity** resulting from electronic charge degrees of freedom and charge ordering (CO). Electric polarization is associated to CO, this ferroelectricity is caused by electron correlation and/or electron-lattice interactions

Ex.: magnetite (Fe_3O_4), perovskite manganites $(PrCa)MnO_3$, 1D and 2D ¼ filled organic salts

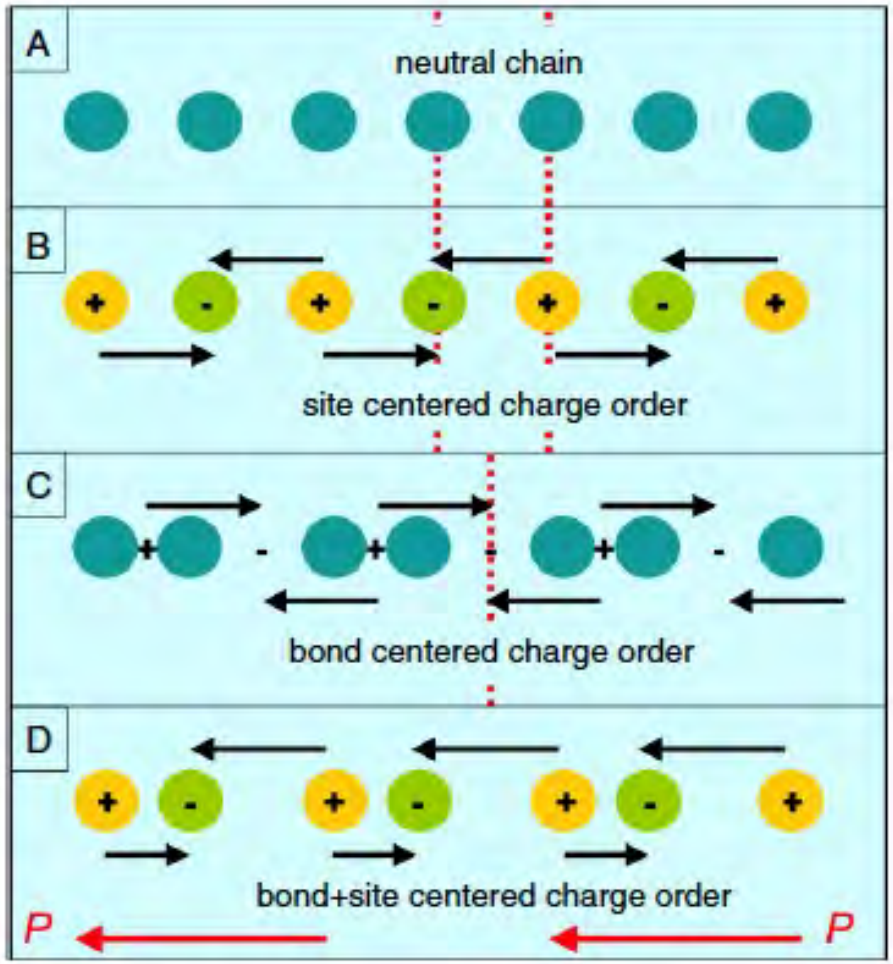

Figure 1. (A) Example of a neutral one-dimensional chain exhibiting (B) site-centered charge ordering, (C) bond-centered charge ordering, and (D) a linear combination of these two that is ferroelectric. The arrows indicate the polarization, which is in total zero in (B) and (C), but develops a macroscopic moment, indicated by the red arrow in (D). The red dashed lines in (A), (B) and (C) indicate mirror planes of the system.

Van der Brink and D.I. Khomskii
JPCM 20, 434217

AC conductivity of $(TMTTF)_2AsF_6$

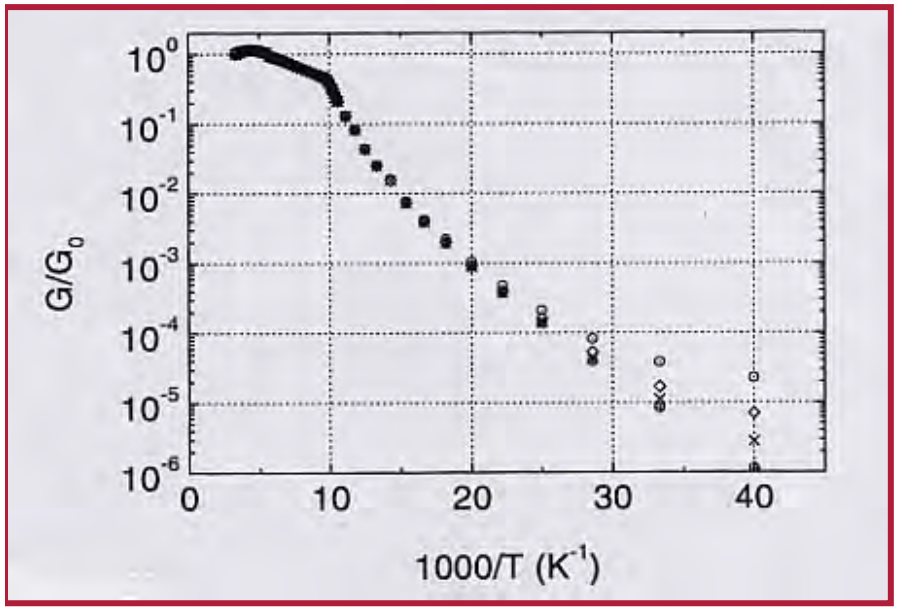

T dependence of the conductance

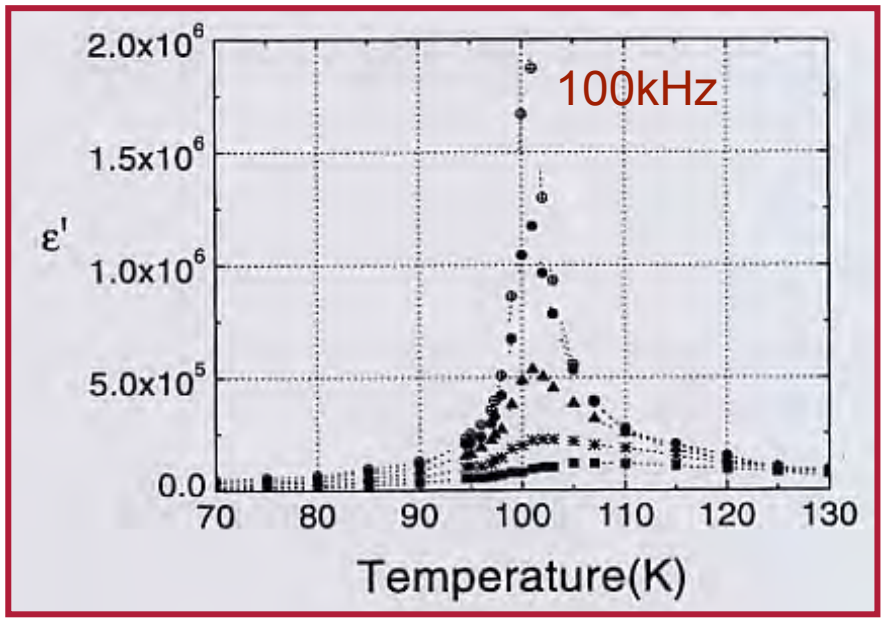

T dependence of the real part of the dielectric permittivity, ε' at 100 et 300kHz, 1,3 and 10MHz

Nad et al.: J. Phys.:Cond. Matter, 12 - L435

Real part of dielectric constant of $(TMTTF)_2X$ salts

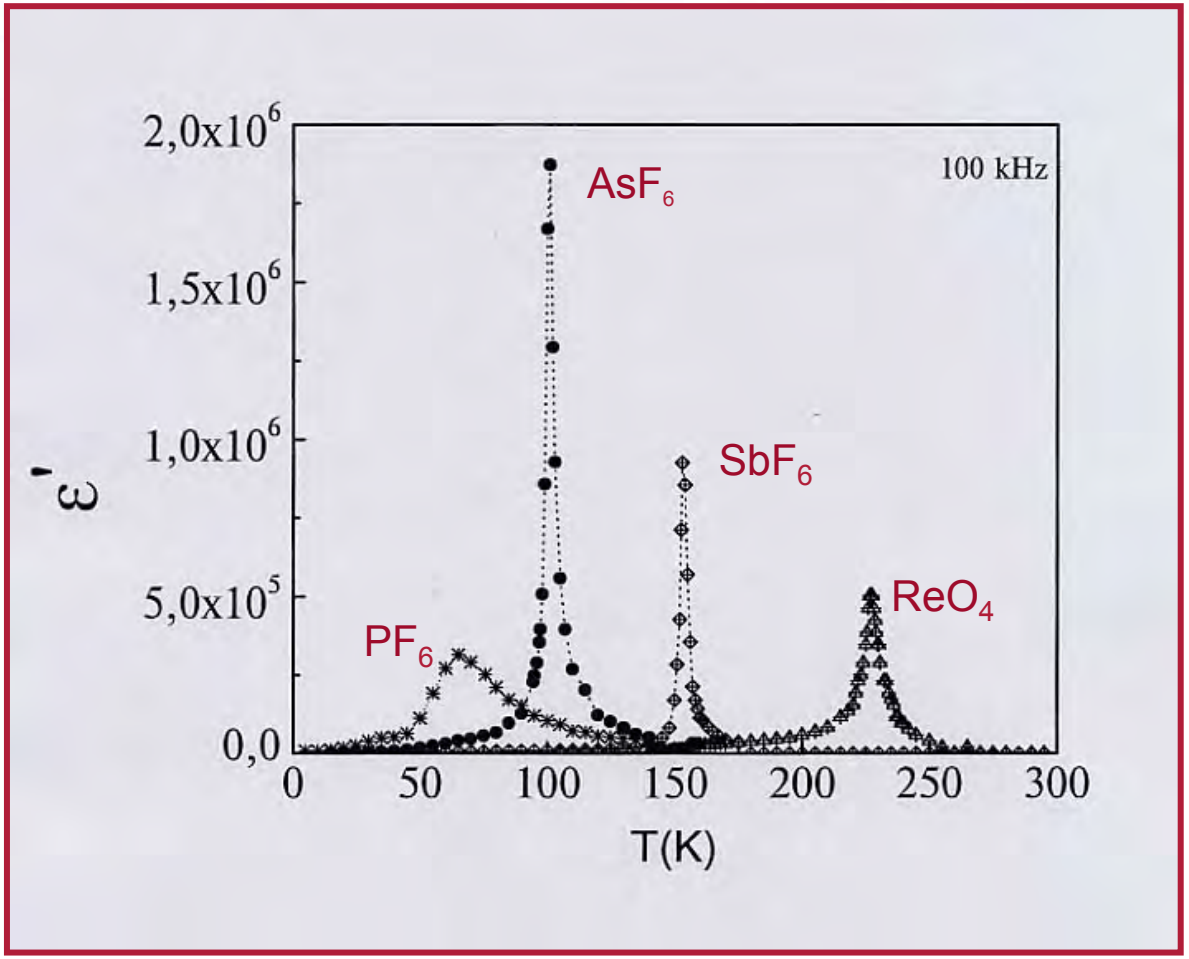

$\varepsilon' = ImG/\omega$

1- For all anions: at $T \approx T_\rho$, there is no anomaly
2- for CSA and ReO_4 anions, ε' diverges at T_{CO}.

Huge magnitudes of ε' : 2.10^6 for AsF_6, 5.10^5 for ReO_4

Charge disproportionation

C^{13} NMR spectra for $(TMTTF)_2AsF_6$

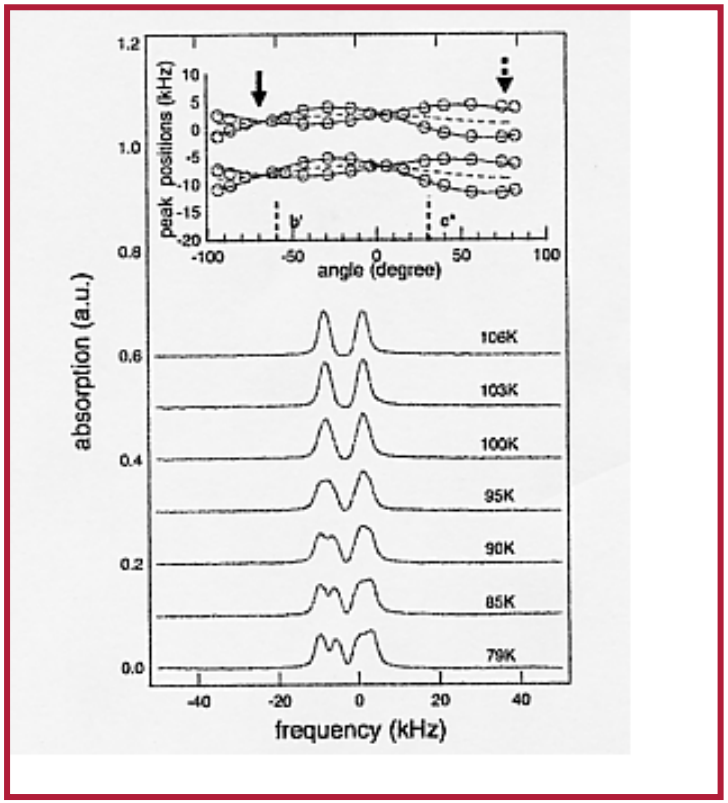

NMR measurements in an external field of 9T (fre 96.4 MHz)

Below T_{CO}, doubling of the spectral line due to two inequivalent molecules with unequal electron densities - Charge disproportionation : 3:1 from T_1^{-1} measurements

Spectral splitting (~charge disproportionation order parameter)versus temperature

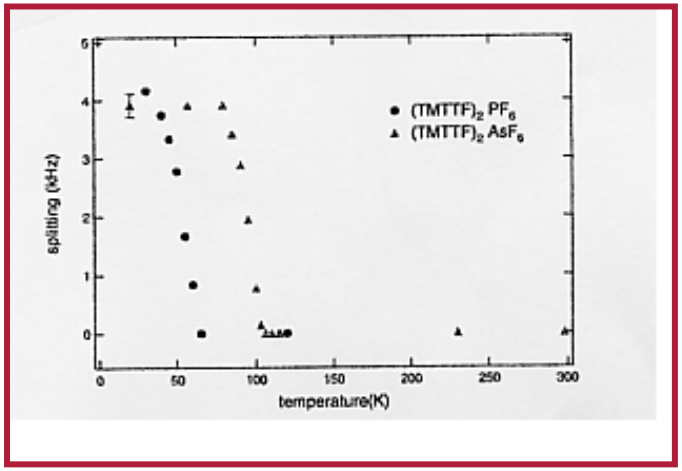

D.S. Chow et al. Phys. Rev. Lett. 85 1698

At high temperatures the unit cell consists of two equivalent TMTTF molecules related by inversion about the counterion.
The breaking of the inversion symmetry within the unit cell below T_{CO}, and the spontaneous dipole moment associated with the charge imbalance on the two molecules yield the ferroelectric behaviour.

Vibrational modes in $(TMTTF)_2X$

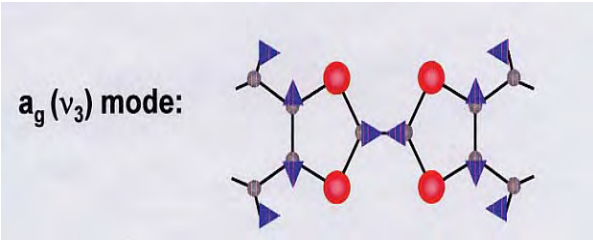

a_g stretching C=C mode: infrared active though electron-molecular (emv) coupling

Neutral TMTTF: $\nu_3 = 1639\ cm^{-1}$ Meneghetti et al.

$TMTTF^+$: $\nu_3 = 1567\ cm^{-1}$ J.Chem. Phys. (1984)

$TMTTF^{0.5+}$: $\nu_3 = 1603 cm^{-1}$

Resonance frequency of emv coupled mode is a function of the charge ($0.5 \pm \rho$) on the molecule

Temperature dependence of the ν_3 mode

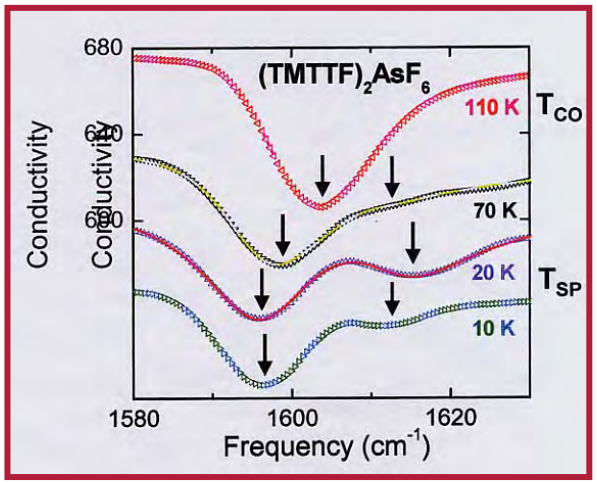

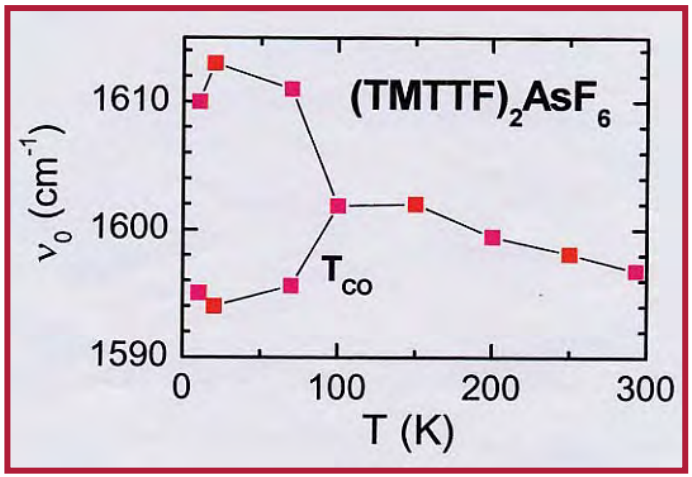

M. Dumm and M. Dressel

AsF_6 T=20K charge disproportionation: +0.63 and +0.37 (2ρ=0.26)

T=10K ------ : +0.60 and +0.40 (2ρ=0.20)

PF_6 T=20K ------ : +0.56 and +0.44 (2ρ=0.12)

Ferroelectric character

The ferroelectric state is triggered by the uniform shift of anions yielding a macroscopic ferroelectric polarization which is gigantically amplified by the charge disproportionation on the molecular stacks (S. Brazovski and T. Nattermann, Adv. in Phys. 53, 177)

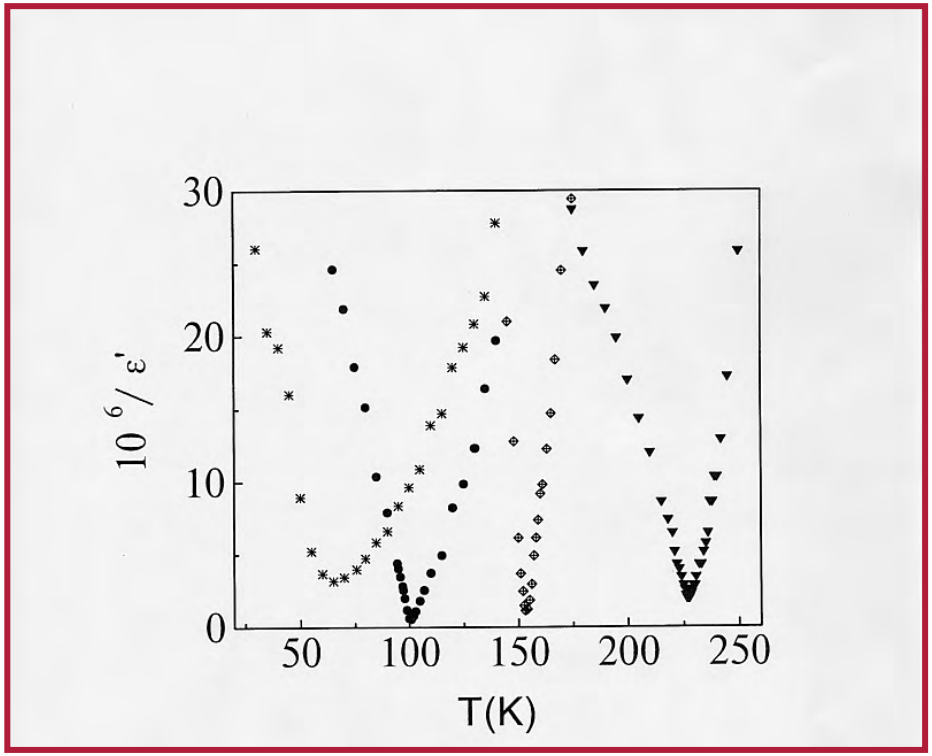

CSA and ReO_4 salts show at T_{CO} a second order phase transition described by the Curie law

$$\varepsilon' = \frac{A}{|T - T_{CO}|}$$

$1/\varepsilon'(T)$ is close to be linear

Ratio A_L / A_H (A_L at $T < T_{CO}$, A_H at $T > T_{CO}$)

in CSA: $A_L / A_H \approx 2$

in ReO_4 $A_L / A_H \approx 1.5$

Phys. Rev. Lett. 86, 4081

2D Quarter-filled Conductors

$(ET)_2X$ compounds

$(ET)_2X$ compounds

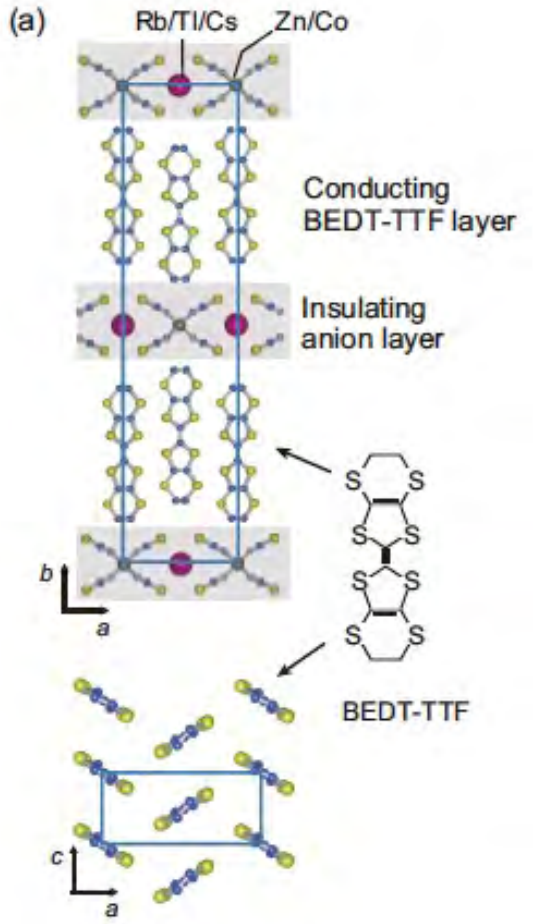

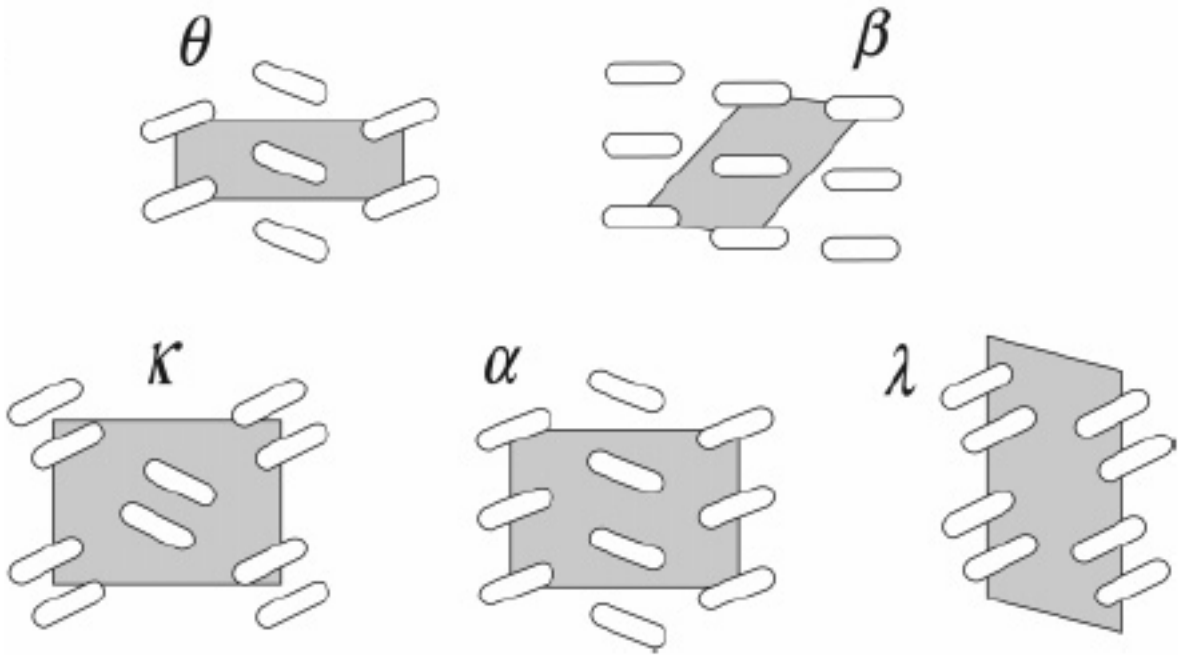

Structures of and θ- $(BEDT\text{-}TTF)_2RbZn(SCN)_4$ and α-$(BEDT\text{-}TTF)_2I_3$

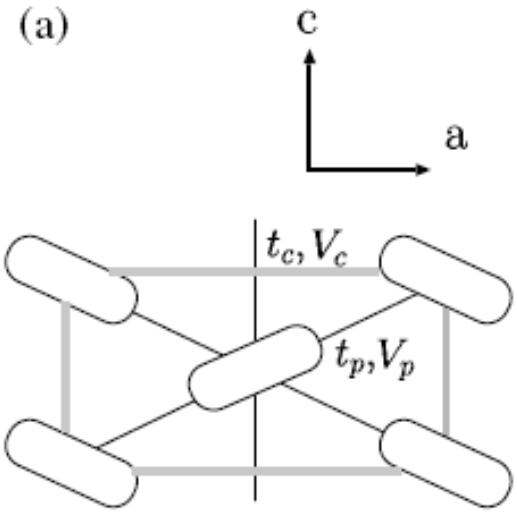

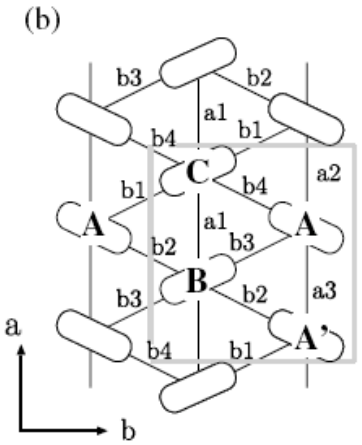

4 (ET) molecules in the unit cell

- Stack 1: A and A' combined by an inversion center
- Stack 2: B and C located on the inversion centers

$$H = \sum_{\langle i,j\rangle\sigma} (t_{ij} c^{\dagger}_{i\sigma} c_{j\sigma} + \text{h.c.}) + U \sum_{i} n_{i\uparrow} n_{i\downarrow} + \sum_{\langle i,j\rangle} V_{ij} n_i n_j$$

Extended Hubbard model in a two-dimensional anisotropic triangular lattice

Y. Tanaka and K. Yonemitsu,J. Phys. Soc. Jpn 79, 024712

Stripe phases

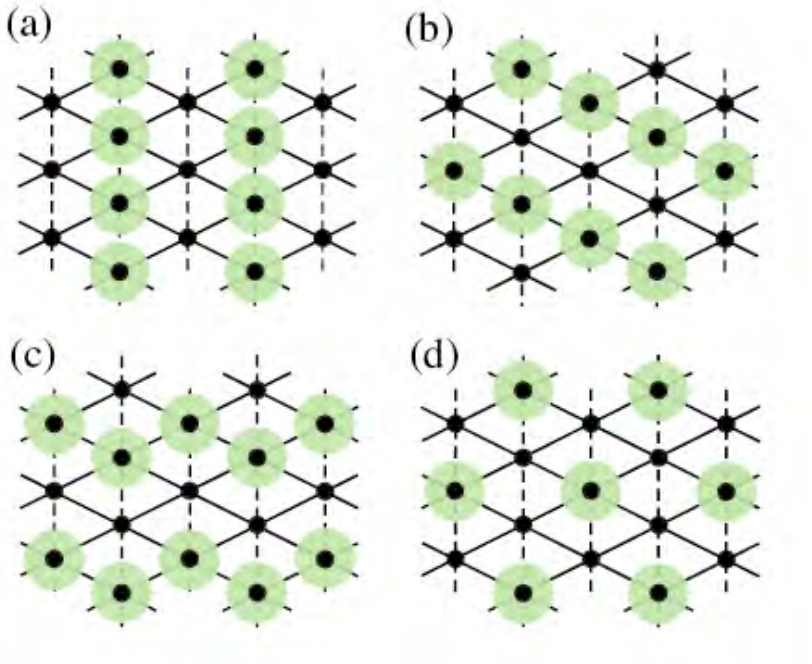

θ- **(BEDT-TTF)$_2$RbZn(SCN)$_4$**

q_1=(1/4, k, 1/3)

q_2 =(0, k, ½)

Different spatial patterns of stripe phases are stabilized depending on the anisotropy of the transfer integrals t_c and t_p and of the values of intersite Coulomb energies along the stacking direction V_c and along the bonds in the transverse direction V_p

-horizontal
-vertical
-diagonal
-3fold

Seo: J. Phys. Soc. Japan 69, 805

Above T_{CO} diffuse rods of modulation vector : **q_1=(1/3, k, 1/4)** around Bragg reflections and diffuse planes connecting these diffuse rods were observed

Below T_{CO}, all diffuse scatterings disappear and replaced by the superlattice reflections with the wavevector **q_2 = (0, k, ½)** [Watanabe et al. J. Phys. Soc. Japan 73, 116]

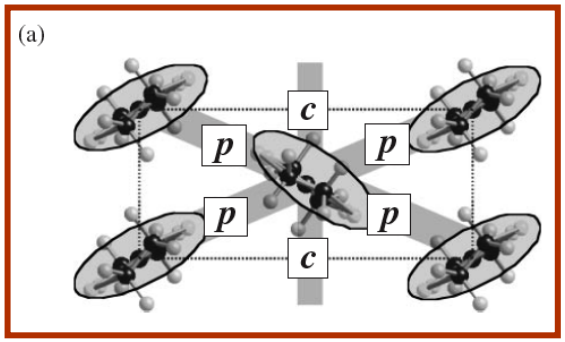

Map of transfert integrals in the a-c plane at 220K

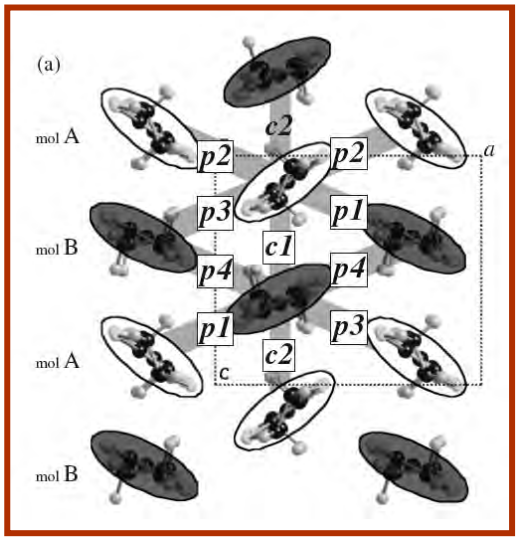

Map of transfert integrals in the a-c plane at 90K

Ionicity of ET molecules determined from bonds lengths
MoleculeA: quasi-neutral (0 to +0.2)
Molecule B: quasi-ionic (+0.8 to 1.0)

⇒Stripe ordering alternating along the c-axis (« horizontal Ordering »).
⇒Uniform 1D spin chains: Bonner-Fisher susceptibility law - Spin-Peierls transition below 25K (dimerization of ET molecules in the 1D chain)

Origin of the triply periodic order indexed by q_1 =(1/4, k, 1/3)?

- Interplay between the Fermi surface nesting and the intersite Coulomb repulsion (Kuroki J. Phys. Soc. Jpn 75, 114716)

- q_1-type modulation comes from the intersite Coulomb repulsion and the q_2-type from the Fermi surface nesting (Odagawa and Motome Phys. Rev. Lett. 98, 206405)

Pin-ball liquid model (Hotta and Furukawa, Phys. Rev.B 74, 193107)

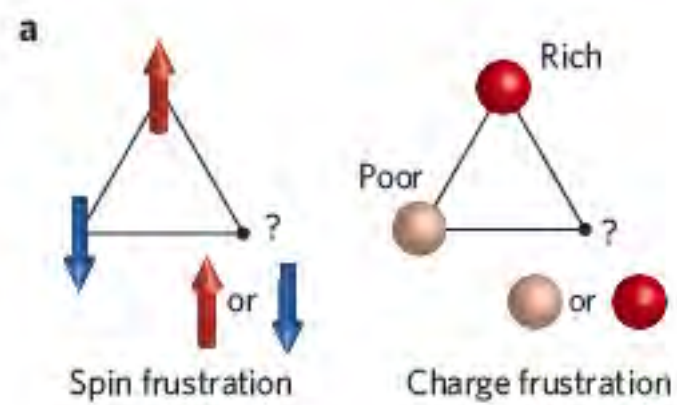

AC conductivity in θ- $(BEDT\text{-}TTF)_2RbZn(SCN)_4$

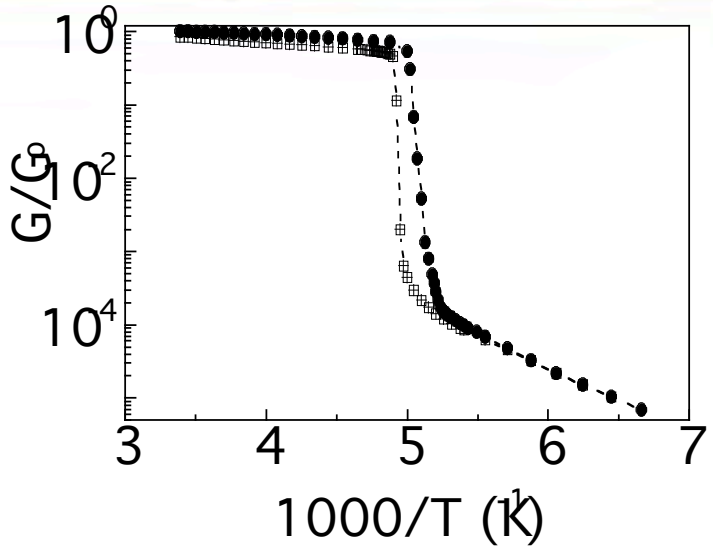

Dependences of the conductance G (at a frequency of 1 kHz) of θ-(BEDT-TTF)RbZn(SCN)$_4$ for slow cooling (triangle) and heating (circles) at a rate of 0.1 K min^{-1} normalized by its value G_o at room tempera-ture as a function of the inverse temperature.

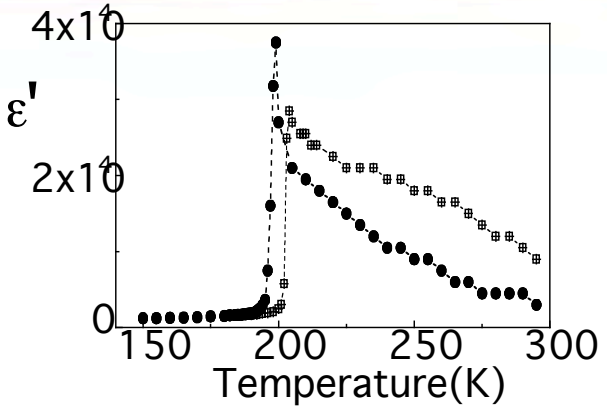

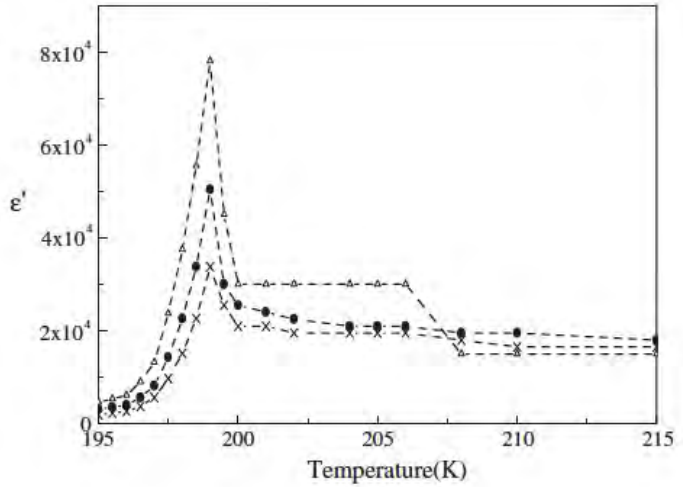

The ε' growth above T_{CO} may indicate the polarizability of the charge disproportionation seen in NMR

The jump below T_{CO} is associated with the 2c superstructure and the large charge gap: T_{CO}= 1900K

Temperature dependence of the real part of the dielectric permittivity ε' of θ-(BEDT-TTF)RbZn(SCN)$_4$ at frequencies of 0.1 (triangles), 1 (circles) and 3 (crosses) MHz at a slow cooling rate 0.1 K min^{-1} in the restricted temperature range in the vicinity of the charge-ordered phase transition.

Nad et al., J. Phys.:Condens. Matter 18, L509

Metal-insulating phase transition in α-(BEDT-TTF)$_2$I$_3$

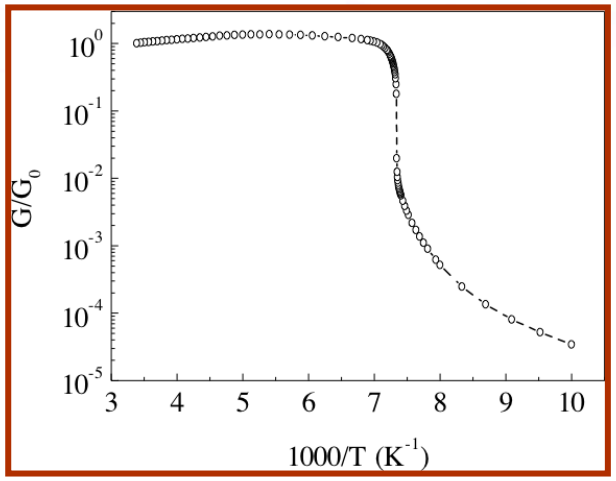

Conductivity

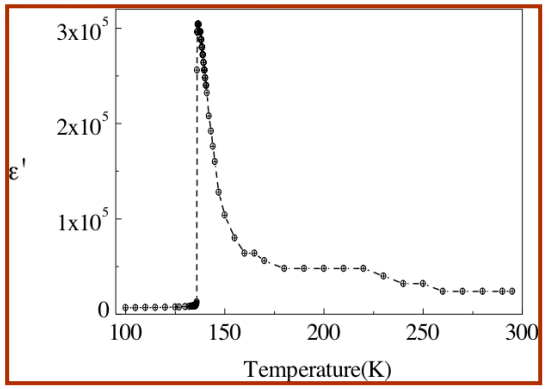

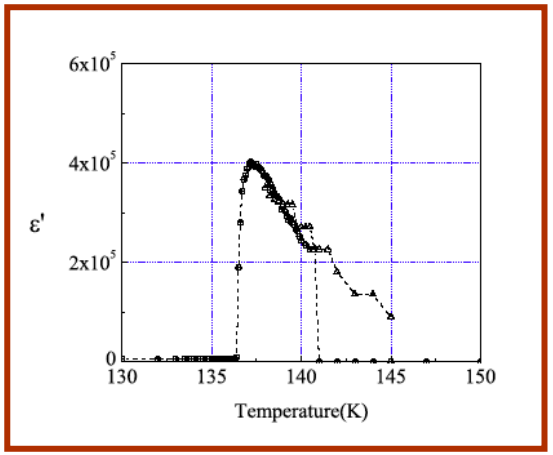

Abrupt phase transition at T=135.1K of first order transition slightly hysteretic

Dimerization of stacks I along the a axis of Peierls type

Drop of ε' below T_{MI}

⇩

Structural transition (dimerization)

Nad et al. Physica B

Charge disproportionation in α-$(BEDT\text{-}TTF)_2I_3$

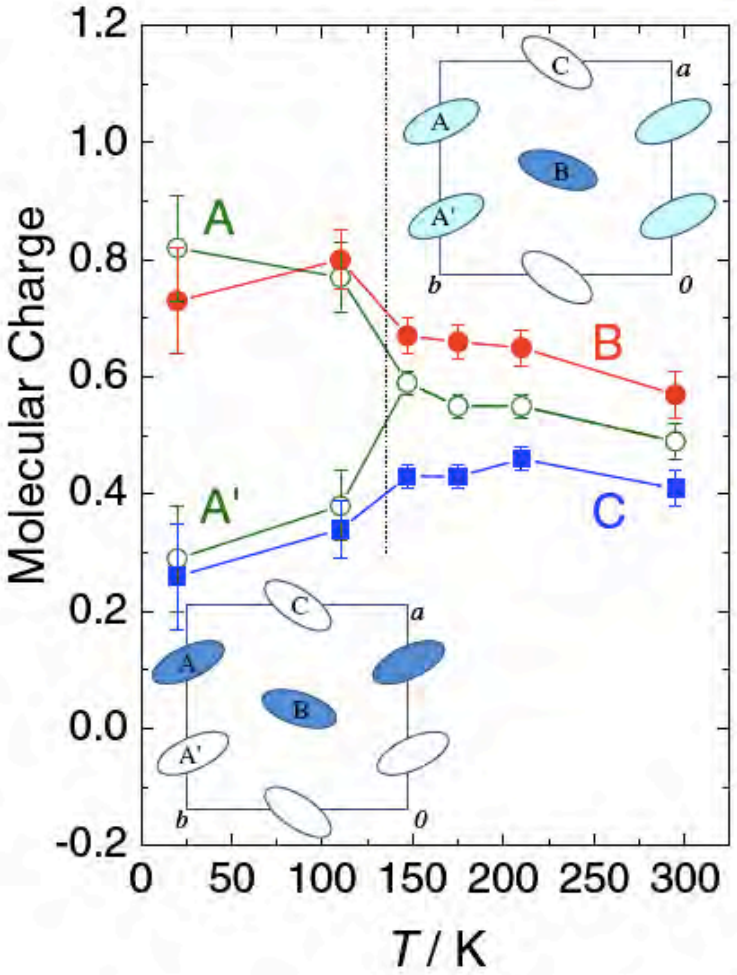

Horizontal stripe structure

CD already above CO transition

From infrared spectroscopy, NMR, and x-ray

At room temperature:
A=A'= 0.60
B=0.68
C=0.44

In the CO state:
A=0.81
A'= 0.26
B=0.74
C=0. 23

T. Kakiuchi et al.
J. Phys. Soc. Jpn 76, 113702

Optical second harmonic generation in α-(BEDT-TTF)$_2$I$_3$

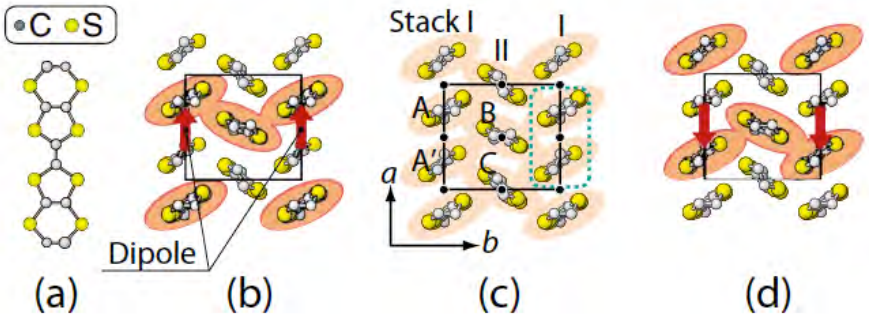

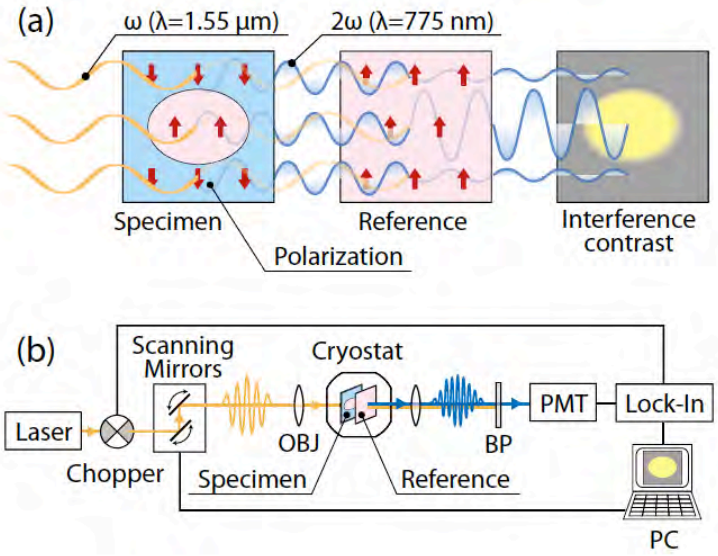

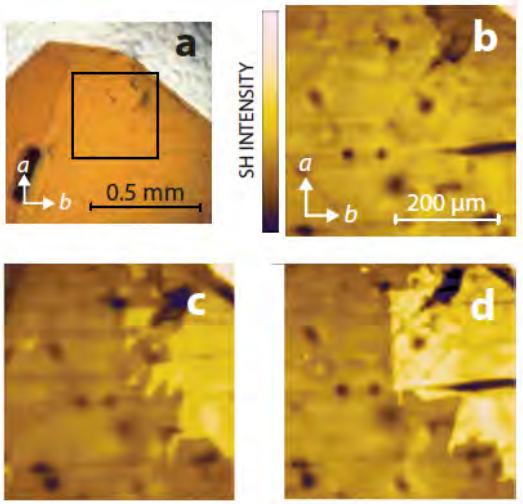

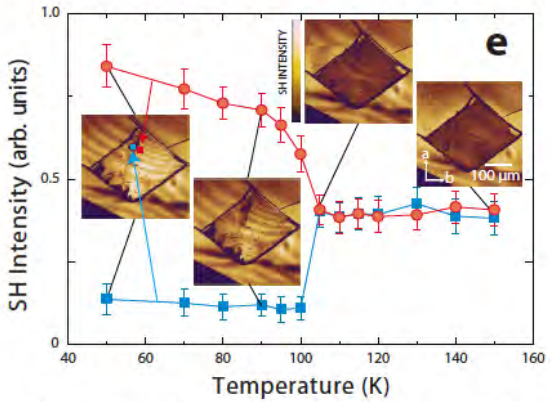

FIG. 3. (Color online) (a) Transmission image of an α-(BEDT-TTF)$_2$I$_3$ crystal. The square indicates the region used for SH observations. SH images measured at (b) 140 K and (c) 50 K. (d) SH image of the same region observed after annealing ($T > T_{CO}$) and afterward slow cooling (T=50 K). (e) SH intensity vs temperature at bright and dark regions in the SH interference image (insets). The fringes appearing the images are the Newton rings caused by an imperfect contact between sapphire plate and the epoxy resin.

Activation of the even-order nonlinear optical phenomenom signifies the lack of inversion symmetry

K. Yamamoto et al. Applied Phys. Letters 96, 122901

SHG Images of $(TMTTF)_2X$ (X = SbF_6, AsF_6, and PF_6)

SbF_6 (as grown)

Transmission Image

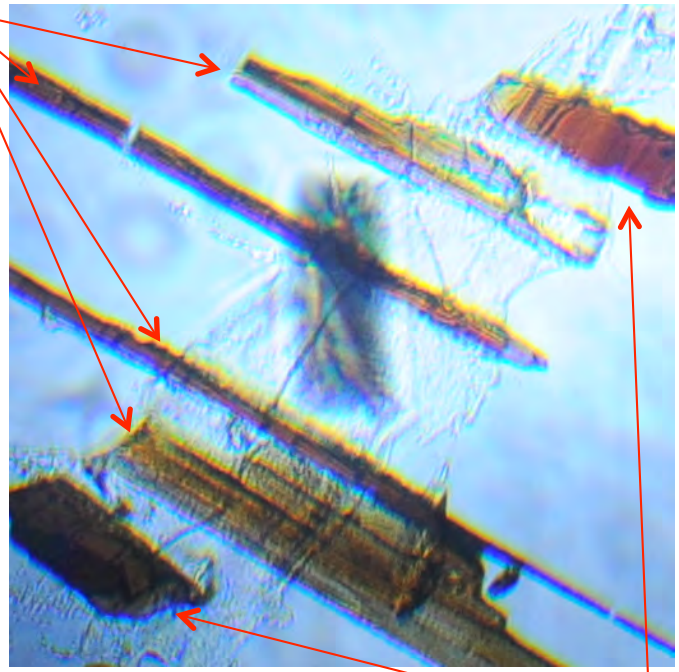

T = RT

SHG Image

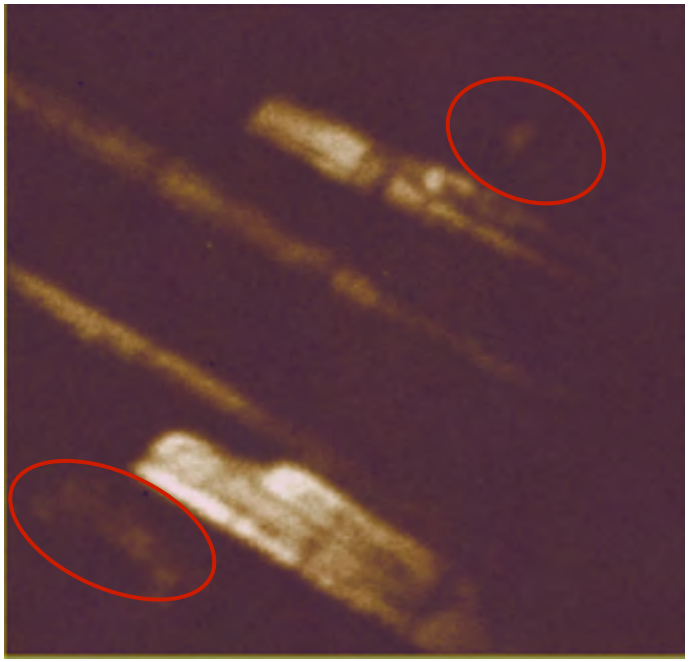

T = 5.7 K

AsF_6 (Cleaved)

K. Yamamoto et al. unpublished

SHG of $(TMTTF)_2X$ (X = SbF_6, AsF_6, and PF_6)

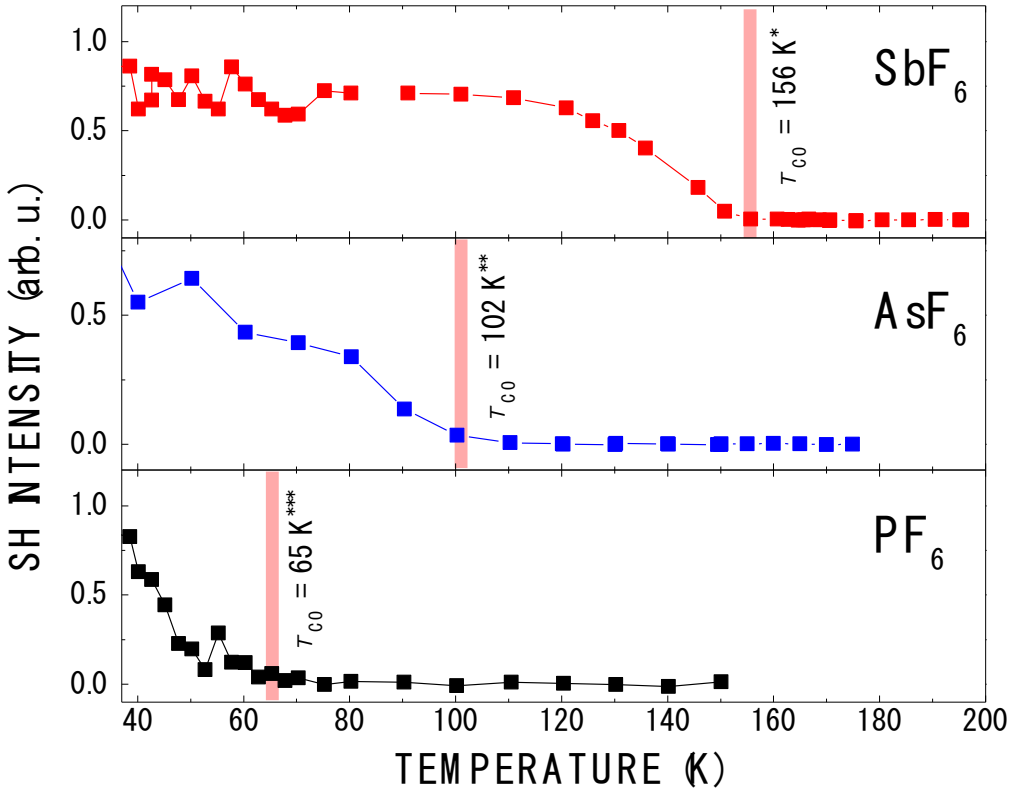

K. Yamamoto et al. unpublished

Effect of cooling rate on the CO in θ- $(ET)_2RbZn(SCN)_4$

1) conductivity

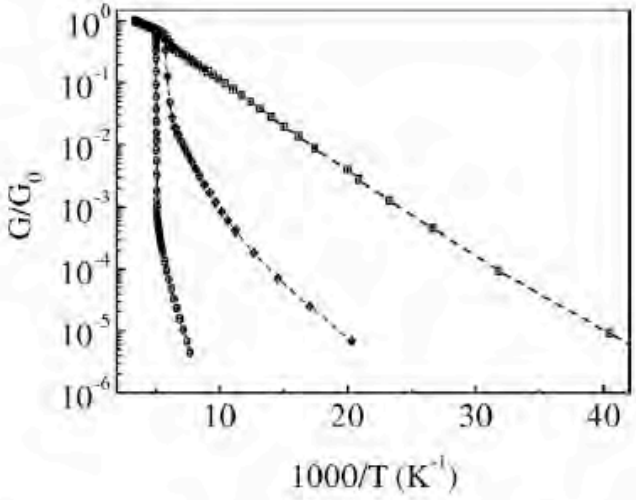

FIG. 2. Variation of the logarithm of the conductance G of θ-$(BEDT\text{-}TTF)_2RbZn(SCN)_4$ normalized by its room-temperature value G_0 as a function of inverse temperature on cooling with three cooling rates: slow (0.1 K/min), intermediate (4 K/min), and fast cooling (9 K/min).

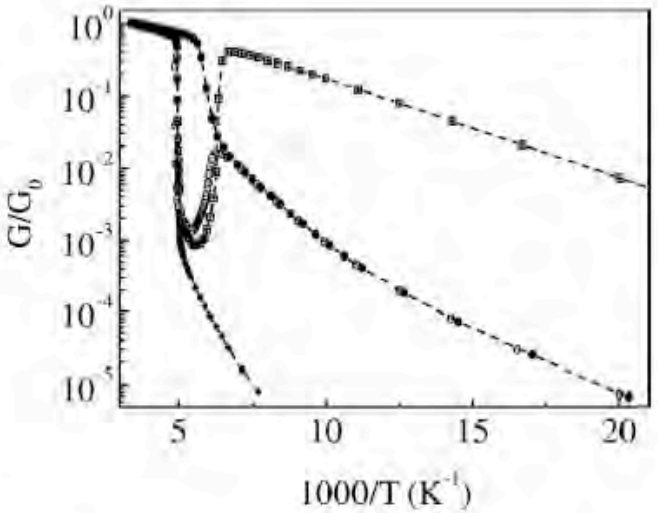

FIG. 3. Variation of the logarithm of the conductance G of θ-$(BEDT\text{-}TTF)_2RbZn(SCN)_4$ normalized by its room-temperature value G_0 as a function of inverse temperature measured on heating from the relaxed, intermediate, and quenched states obtained on cooling with different rates (Figs. 1 and 2). Heating rates: from the relaxed state, 0.1 K/min (◇); from intermediate (◎) and quenched states (□), 4–5 K/min. For comparison, data obtained with intermediate cooling are also shown (●).

F. Nad, PM and H.M. Yamamoto
Phys. Rev. B76, 205101

Effect of cooling rate on the CO in θ- $(ET)_2RbZn(SCN)_4$

2) Dielectric permittivity

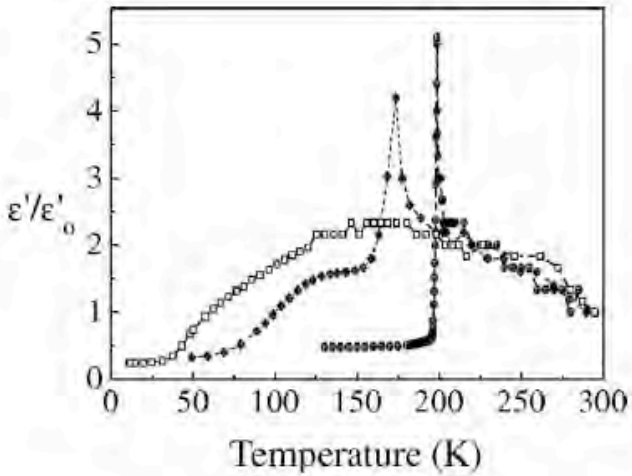

FIG. 4. Variation of the real part of the dielectric permittivity ϵ' of θ-(BEDT-TTF)$_2$RbZn(SCN)$_4$ normalized by its room-temperature value ϵ'_0 as a function of temperature on cooling with three cooling rates: slow cooling at 0.1 K/min, relaxed state (○); intermediate cooling at 4 K/min, intermediate state (◇); and fast cooling at 9 K/min, quenched state (□).

F. Nad, PM and H.M. Yamamoto
Phys. Rev. B76, 205101

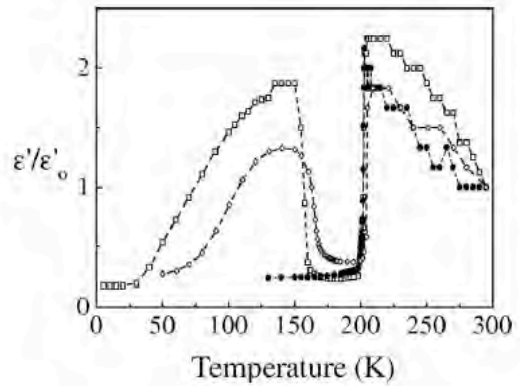

FIG. 5. Variation of the real part of the dielectric permittivity ϵ' of θ-(BEDT-TTF)$_2$RbZn(SCN)$_4$ normalized by its room-temperature value ϵ'_0 as a function of temperature on heating from the relaxed, intermediate, and quenched states obtained on cooling with different rates (Figs. 1 and 2). Heating rates: from the relaxed state, 0.1 K/min (○); from intermediate (◇) and quenched states (□), 4–5 K/min.

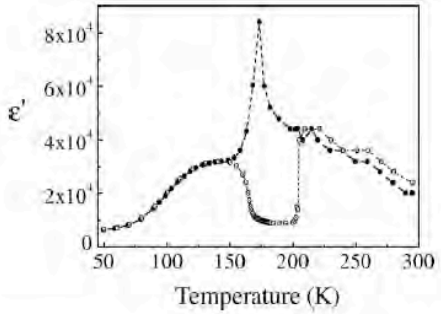

FIG. 6. Comparison of the temperature variation of the real part of the dielectric permittivity ϵ' of θ-(BEDT-TTF)$_2$RbZn(SCN)$_4$ on cooling at the rate 4 K/min (●) and on heating at the rate 4–5 K/min (◎).

Above T_{CO} = 210K, diffuse rods of **q_1=(1/3, k, 1/4)**

Below T_{CO}: **slow cooling:** diffuse rods disappear replaced by **q_2 =(0, k, ½)**

fast cooling: diffuse q_1 remains, but q_2 is disordered in the interlayer direction

similar to θ- $(BEDT\text{-}TTF)_2CsZn(SCN)_4$ at low temperature

↓

Inhomogeneous state composed of q'_1 and q_2 charge order

Charge cluster glass

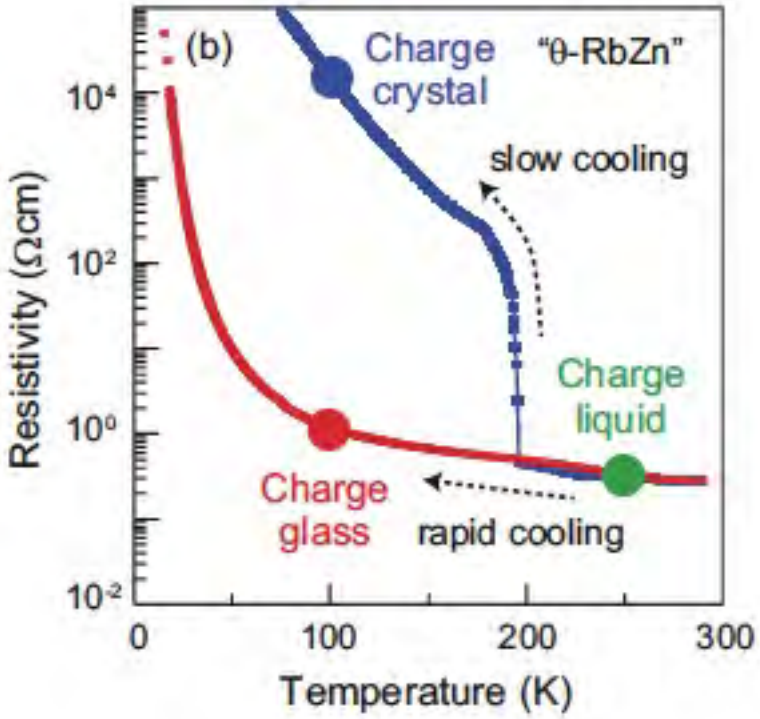

Kagawa et al., Nature Phys. 9, 419

Glass-like state in θ- $(BEDT\text{-}TTF)_2CsZn(SCN)_4$

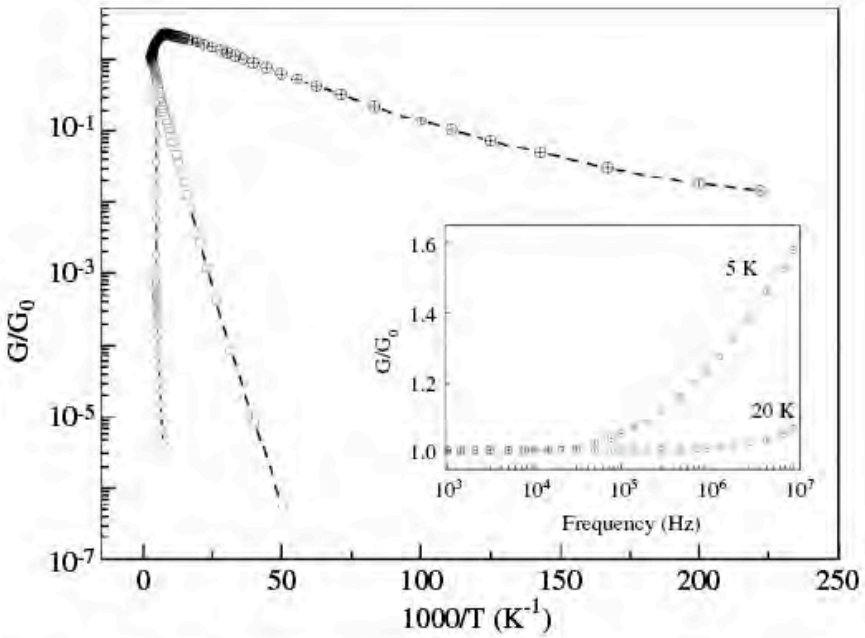

Figure 1. Arrhenius plot of the conductance G, normalized by its room temperature value G_0, at frequency 1 kHz for slow cooling (0.1 K min^{-1}) of θ-$(BEDT\text{-}TTF)_2CsZn(SCN)_4$ (⊕); same plots for θ-$(BEDT\text{-}TTF)_2RbZn(SCN)_4$ with slow cooling (0.1 K min^{-1}) (○) and fast cooling (9 K min^{-1}) (□). The inset shows the frequency dependence of the conductance G of θ-$(BEDT\text{-}TTF)_2CsZn(SCN)_4$ normalized by its value G_0 at two temperatures, 5 and 20 K.

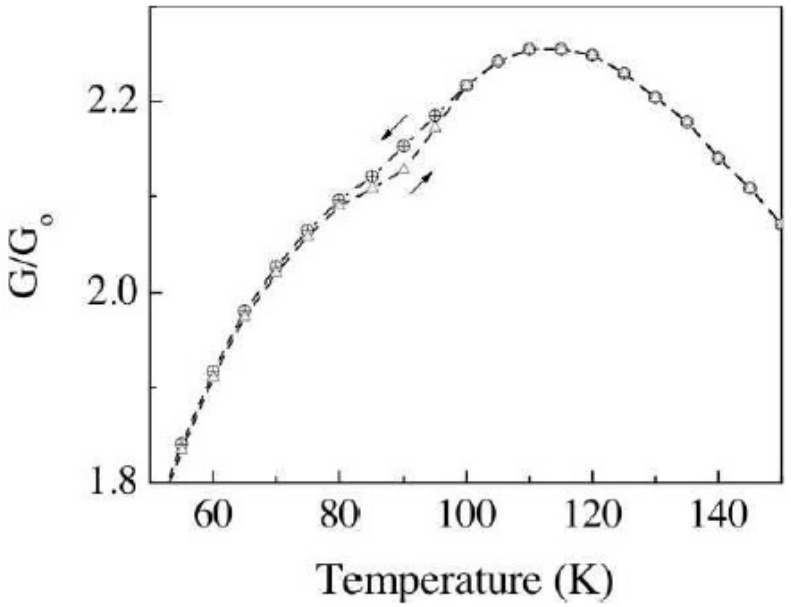

F. Nad, PM and H.M. Yamamoto
J. Phys.: Conden. Matter 20, 485211

θ- $(BEDT\text{-}TTF)_2CsZn(SCN)_4$

$q_1 = (2/3, k, 1/3)$

$q_2 = (0, k, ½)$

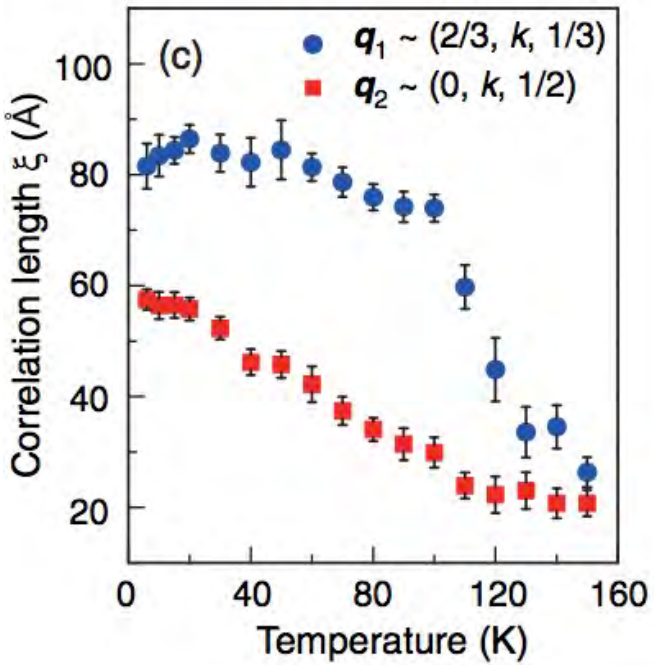

Sato et al., PRB 89, 121102

Both 3x3 and 1x2 period charge clusters are observed in θ- $(BEDT\text{-}TTF)_2CsZn(SCN)_4$
$q_1 = (2/3, k, 1/3)$ and $q_2 = (0, k, ½)$
The size of the q_1 charge clusters grows at T decreases but level off below 100K
while the growth of the q_2 charge clusters continues to grow till much lower temperature

Glass-like state in θ- $(BEDT\text{-}TTF)_2CsZn(SCN)_4$

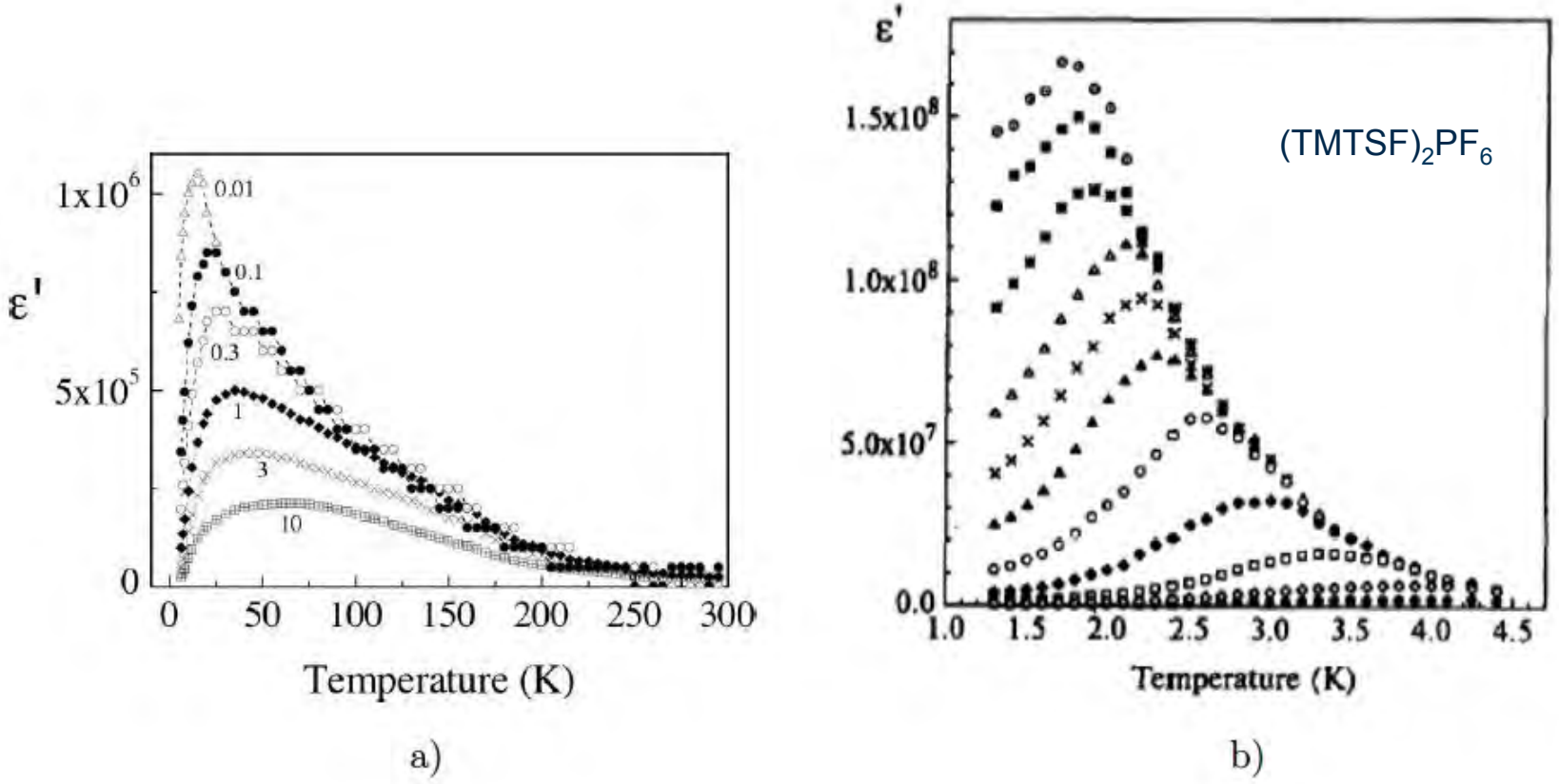

Figure 5. a) Temperature dependences of the real part of dielectric permittivity ϵ' of θ-$(BEDT\text{-}TTF)_2CsZn(SCN)_4$ at different frequencies indicated near the curves in MHz. b) Temperature dependence [36] of the real part ϵ' of $(TMTTF)_2PF_6$ at fixed frequencies (in kHz) top to bottom: 0.111, 0.5, 1.1, 2, 3, 5, 11, 30, 100, 300, 1000.

Comparison between CsZn and fast cooled RbZn

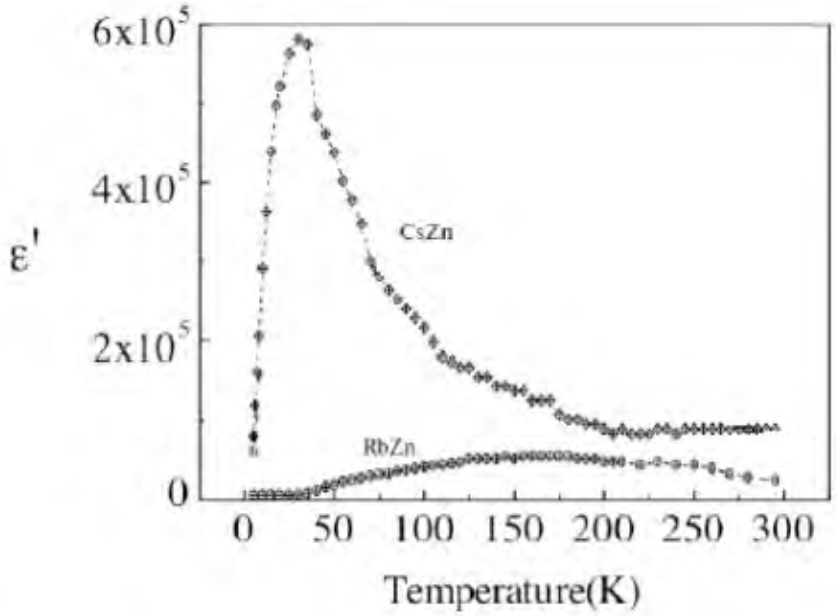

Figure 6. Comparison of the temperature dependence of ϵ' measured at 1 MHz for θ-(BEDT-TTF)$_2$CsZn(SCN)$_4$ and fast cooled (9 K/mn) θ-(BEDT-TTF)$_2$RbZn(SCN)$_4$.

The low temperature of θ- (BEDT-TTF)$_2$CsZn(SCN)$_4$ may indicate a combination of frustated domains which, with decreasing temperature, are frozen into a glass-like short-range charge ordered state

Nonlinear conductivity in α-$(BEDT\text{-}TTF)_2I_3$

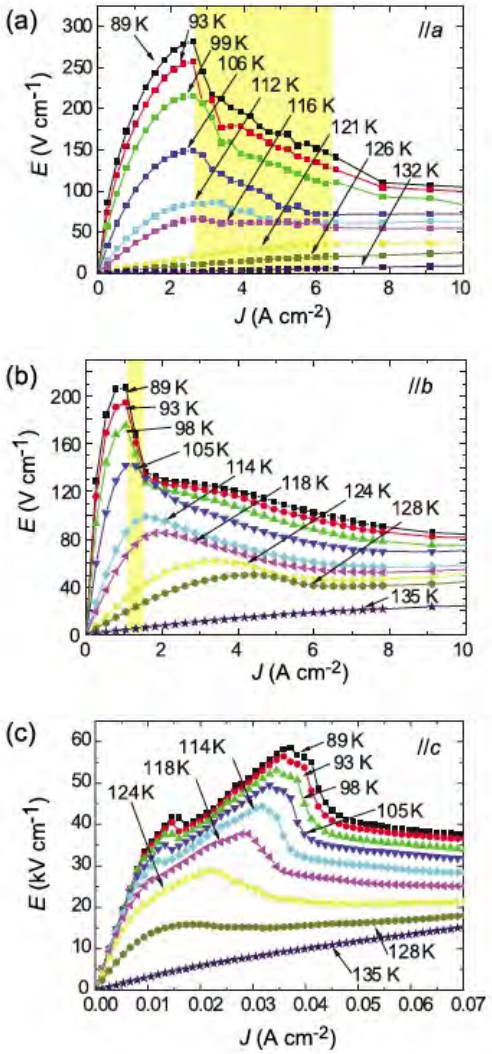

FIG. 2. (Color online) Current-voltage characteristics in α-$(BEDT\text{-}TTF)_2I_3$, measured by applying regulated current pulses along (a) $J \| a$, (b) $J \| b$, and (c) $J \| c$. Oscillation appears in the shaded regions in (a) and (b) at 88 K.

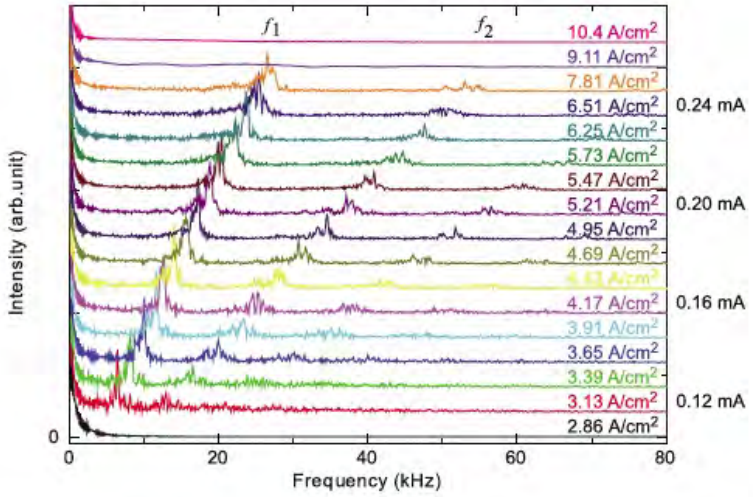

FIG. 4. (Color online) Fast Fourier transformation spectra of the characteristic oscillation observed at 88 K for $J \| a$.

Voltage oscillations in the nonlinear state in the range up to 30kHz

Tamura etal. J. Applied Phys. 107,103716

High field transport from the standpoint of hot electrons

$$nC\frac{dT_e}{dt} = P + \nabla \cdot (K \nabla T_e)$$

$P = \sigma(T_e)\, E^2$ for voltage-regulated scheme

$P = J^2 / \sigma(T_e)$ for current-regulated scheme

The P term gives rise to the energy gain of the electrons and increases electron temperature T_e (C: electron heat capacity

K term gives the spatial distribution of T_e due to thermal conductivity K.

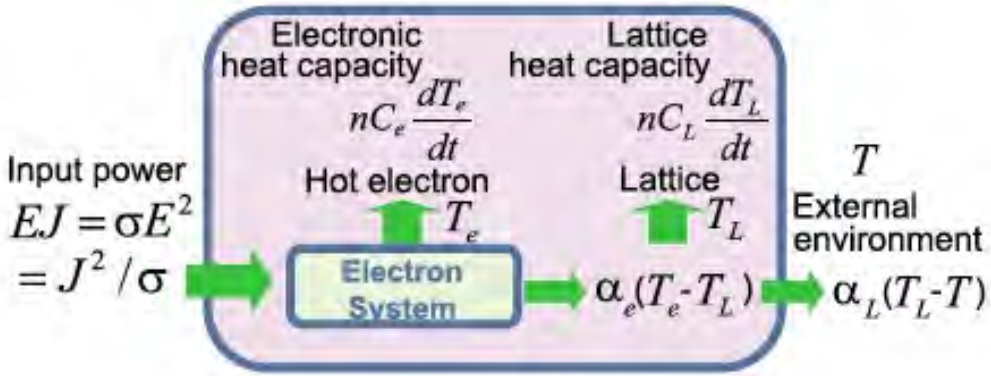

Mori et al. PRB79, 115118

Non linear conduction in rapidly cooled θ- $(ET)_2RbZn(SCN)_4$

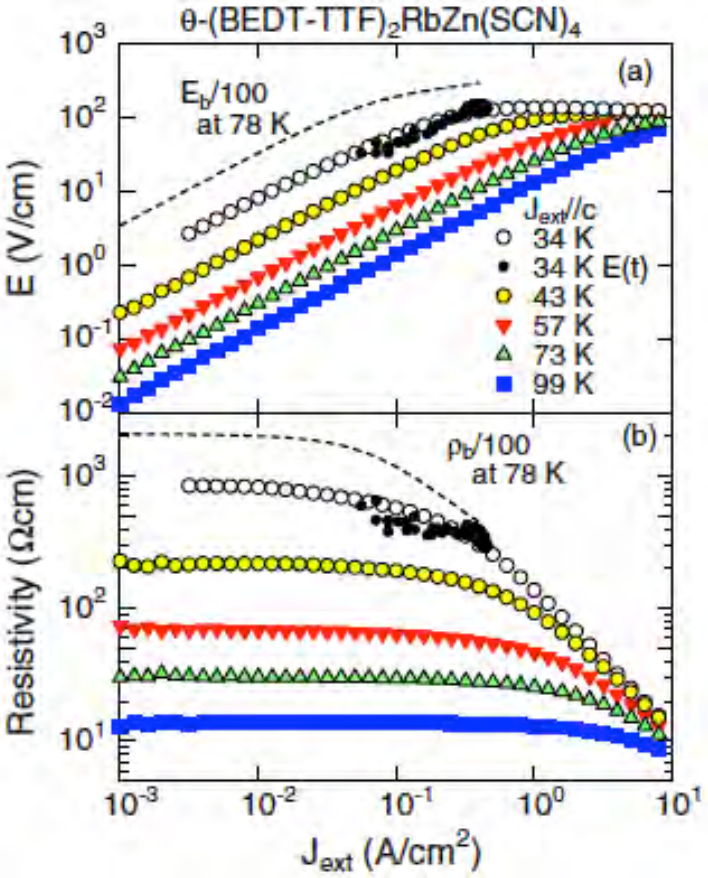

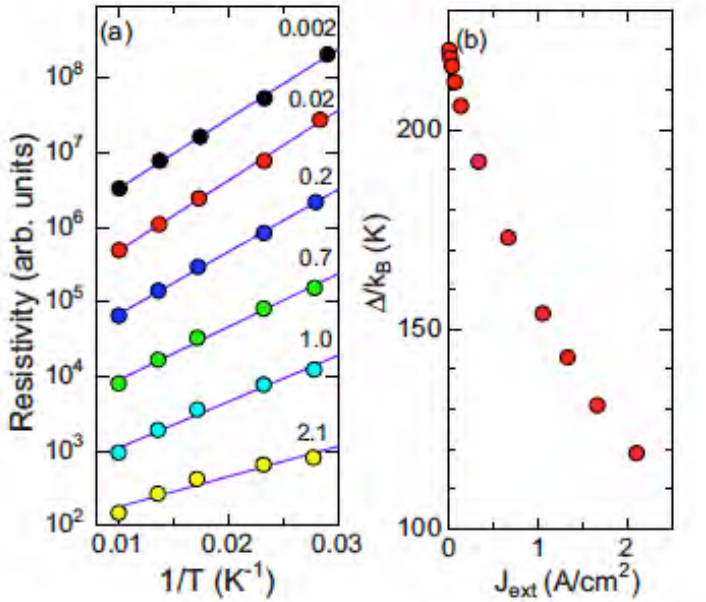

FIG. 4. (Color online) (a) The Arrhenius plots of the resistivity for various current densities J_{ext} indicated by the numbers at the right. Note that each data set is properly shifted to the vertical direction in order to see the change in the slope with J_{ext}. (b) The energy gap obtained from (a) plotted as a function of external current density.

The activation energy Δ decreases roughly linearly with J_{ext}

➔ Flow of carriers may reduce the energy gap order in a nonequilibrium state

Inada et al. Phys. Rev.B79, 165102

Non linear conduction in rapidly cooled θ- $(ET)_2CsZn(SCN)_4$

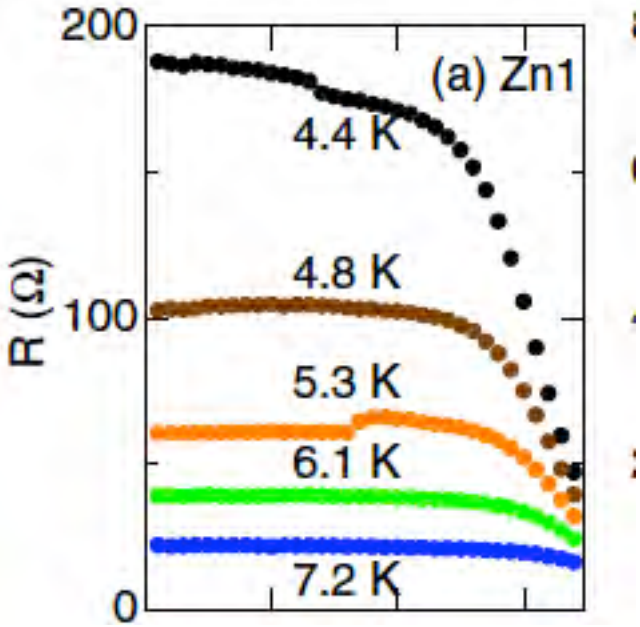

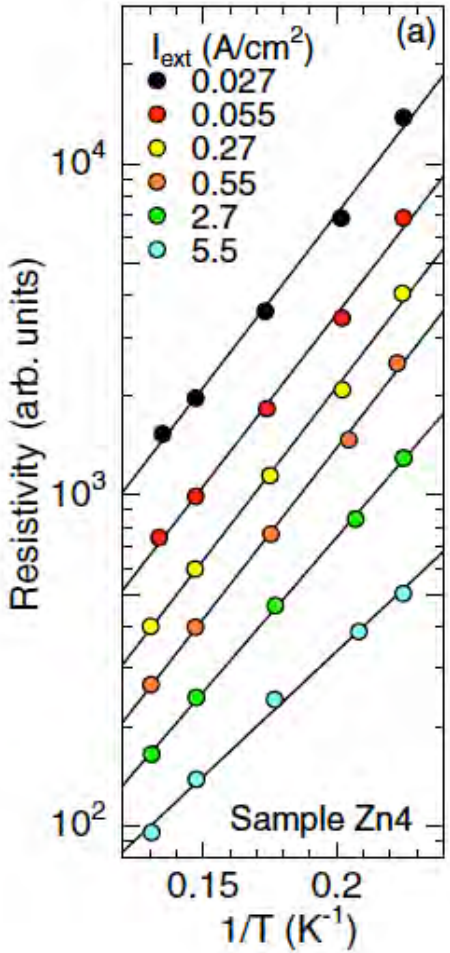

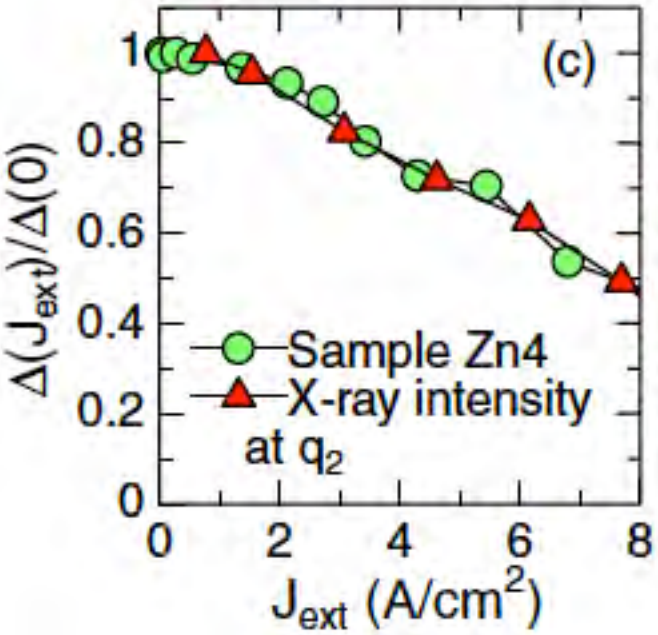

Sawano et al. J. Phys. Soc. Japan 78, 024714

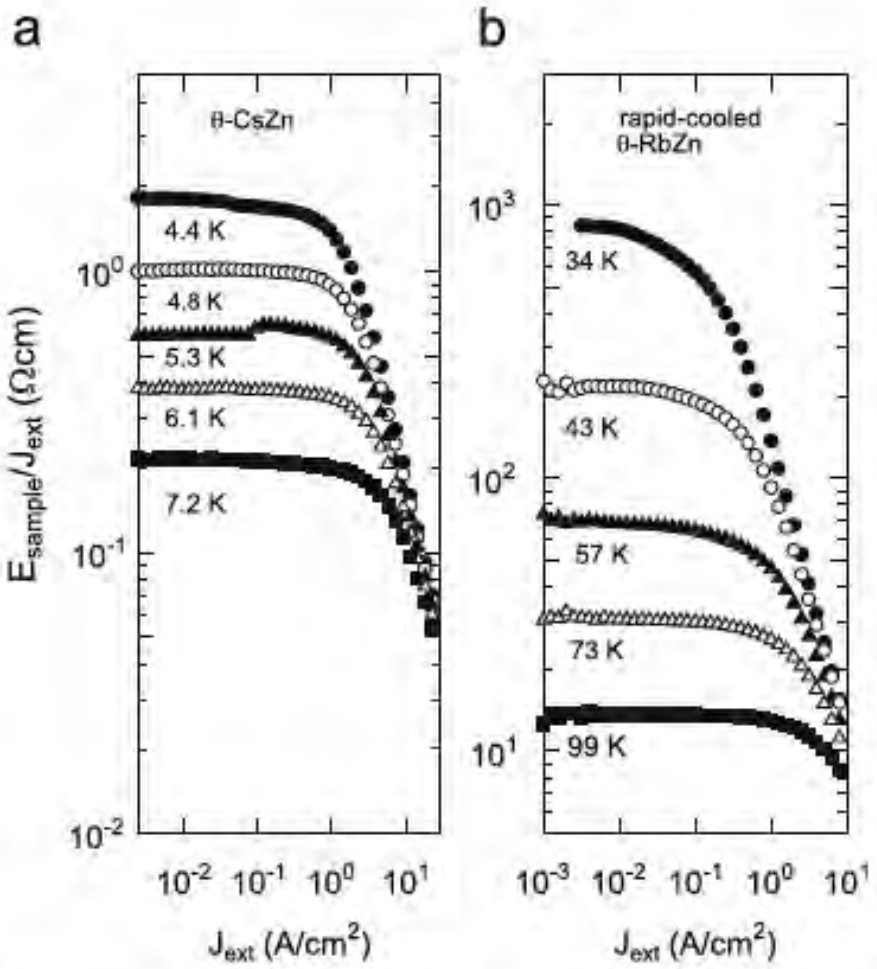

Terasaki et al. Physica B405, S217

Fig. 1. Nonlinear resistivity of the θ–type organic salt along the in-plane direction. (a) θ-(BEDT-TTF)$_2$CsZn(SCN)$_4$ [26] and (b) rapidly cooled θ-(BEDT-TTF)$_2$RbZn(SCN)$_4$ [19].

Similarity with superconductivity where the the energy gap decreases with excess quasiparticule density

Flow of carriers injects extra holes and electrons to the charge-ordered domains and reduce the energy gap in order that the excess carriers are « thermally »activated (Ajisaka et al. Prog. Theor. Phys.121, 1289)

Such a gap reduction is phenomenologically handled by setting an effective temperature T^* higher than T or by setting an effective chemical potential

A different approach for non-linearity

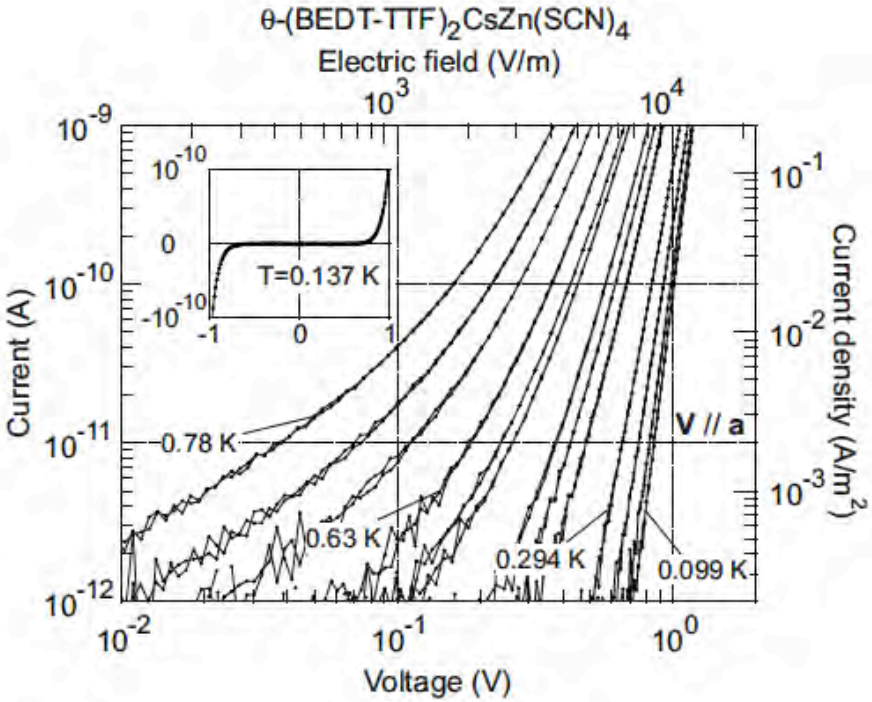

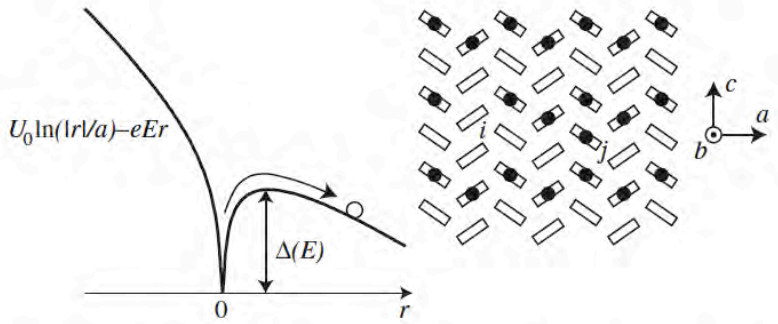

FIG. 3. Left: Schematic drawing of a particle escaping from a tilted logarithmic potential due to thermal activation. Right: Charge-ordered state with an excitation of an electron-hole pair. The boxes represent ET molecules and the dots represent holes.

Nonlinear I-V is attributed to electric field induced unbinding of pairs of a electron and a hole that are thermally excited and attracted to each other due to the 2D long range Coulomb interaction

Takahide et al. Phys. Rev. 81, 235110

Current-induced melting of the charge order in CsZn

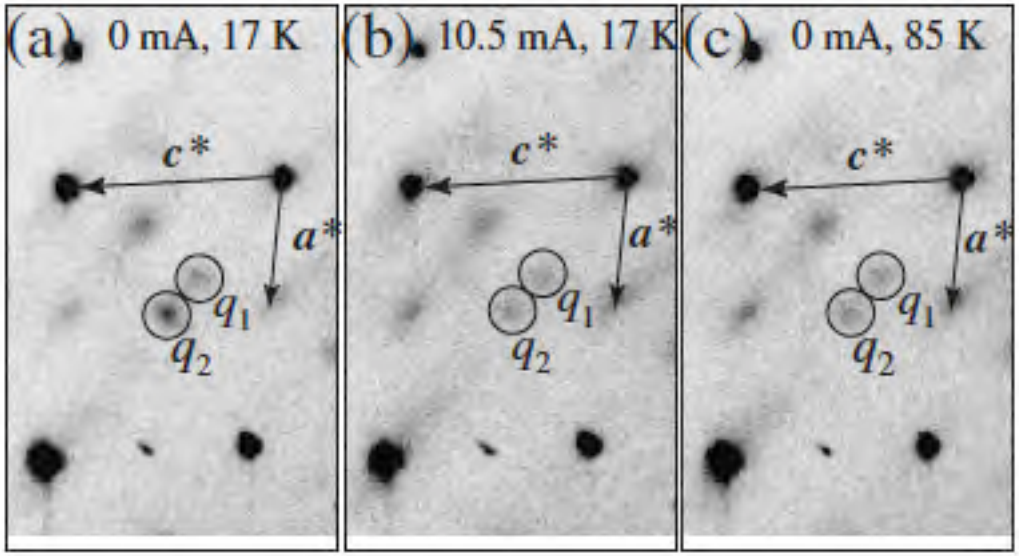

M. Watanabe et al.
J. Phys. Soc. Jpn, 77, 065004

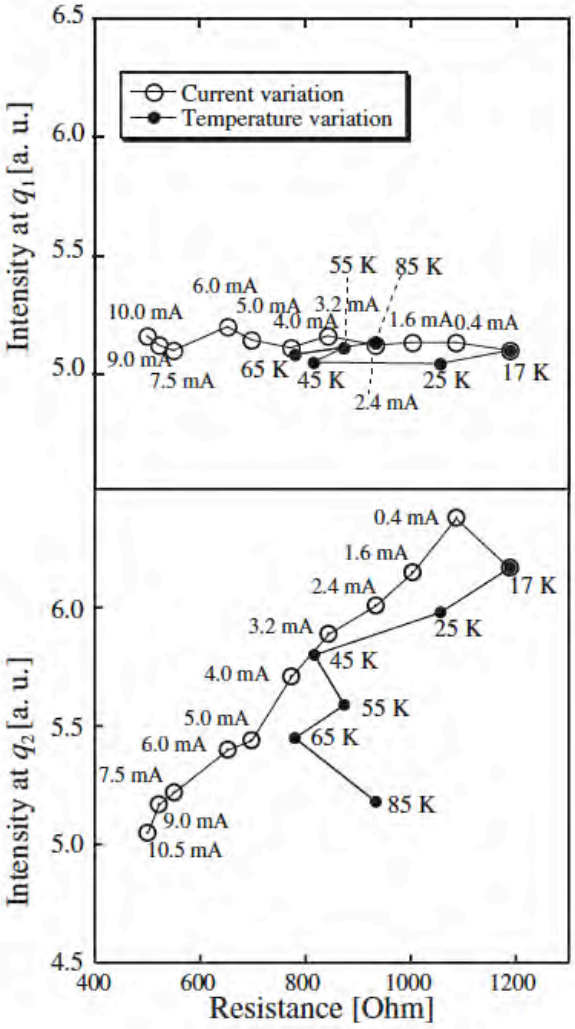

q_1=(2/3, k, 1/3)
q_2 =(0, k, 1/2)

With external current, only the two-fold ordering melts

The nonlinear conduction is induced by the CO melting with charge flow

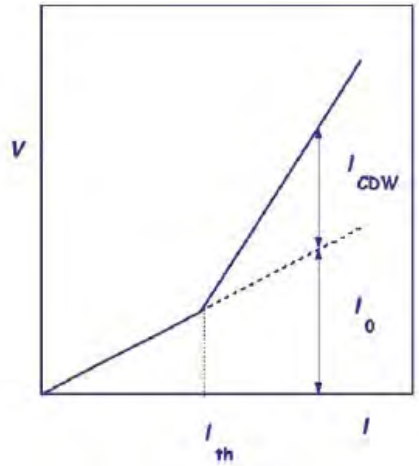

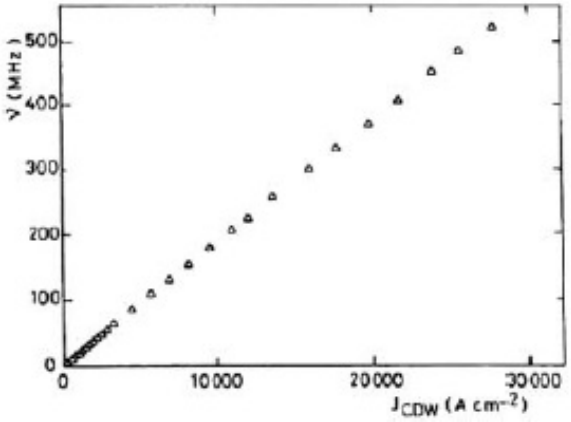

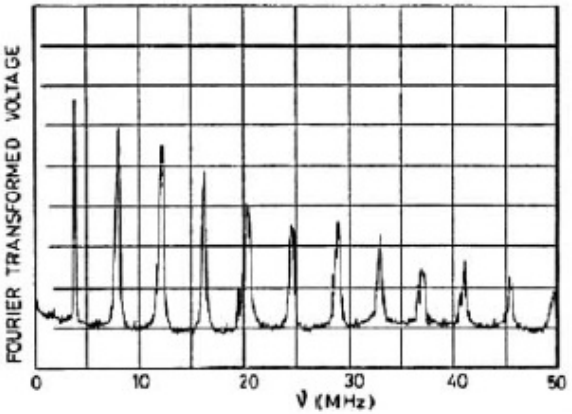

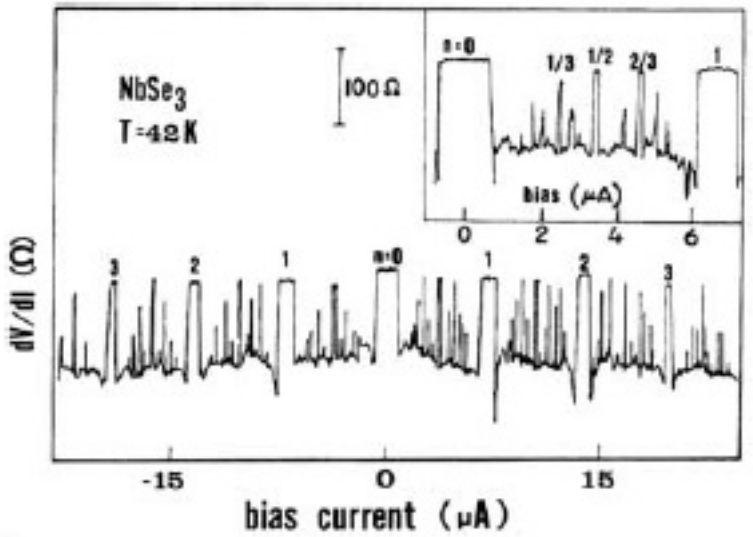

$$J_{CDW} = ne\frac{2\pi}{Q}v = ne\,\lambda_{CDW}v.$$

Electronic crystals: an experimental overview
PM, Adv. In Phys. 61 (2012) 325

Conclusions

-the combination of site-centered and bond-centered charge order yields ferroelectricity as seen in 1D organic salts

-in 2D (BEDT-T) salts, the stabilization of charge order takes place with the doubling of the unit cell in slow cooling process and with the tendency of the divergence of the dielectric permittivity

In θ- $(ET)_2RbZn(SCN)_4$, dimerization is suppressed by fast cooling

In θ- $(ET)_2CsZn(SCN)_4$ there is no long range charge order state but competition between two superstructures which induces glassy state at low temperature

-For nonlinearity, the energy gap of the charhe order decreases with excess injected quasi particules which are thermally activited (thermal model)
Very surprinsingly nonlineratity occurs with melting of the two-fold superstructure

Acknowledgements for samples

J. M. Fabre
Laboratoire de Chimie Organique, Montpellier, France

MT. Nakamura and K. Furukawa
Institute for Molecular Science, Okazaki, Japan

H. Müeller
ESRF , Grenoble, France

H. M. Yamamoto
Riken, Saitama, Japan

K. Yamamoto
Institute for Molecular Science, Okazaki, Japan